Journal of Human Evolution 98 (2016) 36–65

Contents lists available at ScienceDirect

Journal of Human Evolution

journal homepage: www.elsevier.com/locate/jhevol

In vivo bone strain in the mandibular corpus of *Sapajus* during a range of oral food processing behaviors

Callum F. Ross [a, *], Jose Iriarte-Diaz [b], David A. Reed [b], Thomas A. Stewart [a], Andrea B. Taylor [c]

[a] Department of Organismal Biology & Anatomy, The University of Chicago, United States
[b] Department of Oral Biology, College of Dentistry, University of Illinois at Chicago, United States
[c] Department of Community and Family Medicine, Duke University, United States

ARTICLE INFO

Article history:
Received 24 July 2014
Accepted 25 June 2016
Available online 23 August 2016

Keywords:
Cebus
Capuchin monkeys
Mastication
Ingestion
Mandibular biomechanics
Feeding ecology

ABSTRACT

It has been hypothesized that mandibular corpus morphology of primates is related to the material properties of the foods that they chew. However, chewing foods with different material properties is accompanied by low levels of variation in mandibular strain patterns in macaques. We hypothesized that if variation in primate mandible form reflects adaptations to feeding on foods with different material and geometric properties, then this variation will be driven primarily by differences in oral food processing behavior rather than differences in chewing per se. To test this hypothesis, we recorded in vivo bone strain data from the lateral and medial surfaces of the mandibular corpus during complete feeding sequences in three adult male *Sapajus* as they fed on foods with a range of sizes and material properties. We assessed whether variation in mandibular corpus strain regimes is associated with variation in feeding behaviors and/or chewing on different foods, and we quantified the relative variation in mandibular corpus strain regimes associated with chewing on foods of different material properties versus a range of oral food processing behaviors (incisor, premolar, and molar biting; pulling on incisors; mastication). Feeding behavior had a significant effect on mandibular corpus strain regimes, as did chewing side and the cycle number in a feeding sequence. However, food type had weaker effects and usually only through interaction effects with chewing side and/or cycle type. Strain regimes varied most across different chew sides, then across different behaviors, and lastly between mastication cycles on different foods. Strain magnitudes associated with premolar, molar, and incisor biting were larger than those recorded during mastication. These data suggest that intra- and inter-specific variation in mandible morphology is a trade-off between performance requirements of different oral food processing behaviors and of variation in chewing side, with direct effects of food type being less important.

1. Introduction

The relationship between diet and mandible morphology in primates is poorly understood. Dietary category (e.g., folivory, frugivory) and food material properties (FMPs; e.g., toughness, Young's modulus) have been hypothesized to be functionally related to the shape of the primate mandibular corpus (Beecher, 1977, 1979; Hylander, 1979b, 1988; Bouvier, 1986a, b; Ravosa, 1991, 2000; Wallisch et al., 2009). However, these relationships are not consistent across primate clades, suggesting that it is not just dietary category and FMPs that drive form-function relationships in primate mandibles (Ross et al., 2012; Ross and Iriarte-Diaz, 2014). Primates engage in a wide range of feeding and non-feeding behaviors that place varying demands on the mandible (Smith, 1984; Daegling, 1992, 1993, 2002, 2007; Daegling and Grine, 2006; Daegling and McGraw, 2007; Terhune et al., 2011; Ross et al., 2012; Hylander, 2013; Ross and Iriarte-Diaz, 2014). These include pre-ingestive and ingestive food processing behaviors such as gouging, stripping, peeling, husking, incisor biting, premolar biting, and molar biting, as well as intra-oral food transport, food manipulation, mastication, and swallowing. Important non-food processing behaviors employing the mandible include yawning, licking, drinking, grooming, agonistic threat displays, and vocal communication.

* Corresponding author.
E-mail address: rossc@uchicago.edu (C.F. Ross).

http://dx.doi.org/10.1016/j.jhevol.2016.06.004
0047-2484/

The relative importance of performance of these different behaviors for mandibular form is unknown. Some behaviors such as vocalization, yawning, licking, threat displays, and drinking elicit low bone strain magnitudes in the mandible and are therefore assumed to be less important determinants of aspects of primate mandibular form related to its mechanical strength than is feeding (Hylander, 1979c, 1984) although for a contrasting opinion see (Daegling, 2012). In contrast, bone strain magnitudes in the mandibular corpus and symphysis recorded when animals bite on a force transducer with their incisors, premolars, and molars can be relatively high, and often higher than those recorded during mastication (Hylander, 1979c, 1984; Ross and Metzger, 2004). This suggests that an evaluation of bone strain regimes in the mandible during a broad range of feeding behaviors might be informative about the determinants of mandibular form. The phrase "feeding behavior" has been used to refer to a wide range of behaviors, from general behaviors such as grazing, browsing, "high selectivity," and "low selectivity" (Van Soest, 1996) to specific gape cycle types, such as chewing, gnawing, and swallowing (Hiiemae, 2000: 244; see Ross and Iriarte-Diaz [2014] for a recent review of the hierarchical levels of feeding behavior terminology in primate feeding biomechanics and ecology.) In this study, we focus on a range of behaviors that we define as *oral food processing behaviors*, including incisor, premolar, and molar biting, pulling on incisors, and mastication, behaviors during which mechanical forces are applied to food items through the mandible, accompanied by jaw muscle forces and reaction forces acting on the mandible from the food item, teeth, and jaw joints (e.g., Hiiemae, 1976, 1978).

1.1. Is variation in mandibular corpus morphology related to variation in what primates masticate/chew?

One possibility is that interspecific variation in mandibular shape, as estimated by external dimensions of the mandibular corpus, does not reflect adaptation to variation in the *nature* of mandibular stress, strain, and deformation when chewing different foods (see Table 1 for definitions), but adaptation to variation in the amount of strain (some integral of strain magnitude and/or number of cycles) associated with chewing. For example, Hylander (1979b) suggested that mastication might influence mandible morphology through selection to improve mandibular resistance to bone fatigue. Noting that the mandibular corpora of colobines are deeper than those of related cercopithecines, that most colobines are highly folivorous, and that leaves require more masticatory cycles than fruit, Hylander (1979b: 230) hypothesized that the relatively deeper mandibular corpora of colobines might function to "prevent mandibular bone fatigue due to cyclical repetitious bending loads." This hypothesis then was applied to explain patterns of mandibular variation between grass-eating cercopithecines (gelada baboons) and frugivorous cercopithecines (Hylander, 1979b), across living and fossil prosimians (Ravosa, 1991, 1992, 2007), an extensive sample of cercopithecoids (Ravosa, 1996), and apes (Ravosa, 2000; Taylor, 2002, 2006a, b).

Another possibility is that interspecific differences in mandible morphology reflect differences in the *nature* of mandibular loading, stress, and strain regimes associated with mastication of different foods. In macaques, mastication of different foods (apple, dried peach, celery) elicited different orientations of principal strains (ε_1, ε_2; different strain regimes) on the lateral aspect of the balancing side mandibular corpus (Fig. 1; Hylander, 1979c: Table 10). Moreover, mastication on different foods elicits differences in relative amplitude and timing of activation of jaw elevator muscles (Hylander and Johnson, 1994). The jaw elevator muscles apply large external forces to the mandible during the power stroke of mastication, so variation in their activity associated with mastication of different foods might be associated with variation in mandibular strain, stress, and deformation regimes. Moreover, because the orientation of the bite reaction force acting on the mandible is a function of both dental occlusal morphology and the direction of jaw movement during occlusion (Hildebrand, 1931; Beyron, 1964; Ingervall, 1972; Suit et al., 1976; Woda et al., 1979; Ekfeldt and Karlsson, 1996; Rilo et al., 2009), the variation in occlusal morphology between different primates might result in different bite force orientations during the power stroke of mastication, which in turn could result in, for example, different twisting moments acting on the corpus (Hylander, 1979b, 1988).

Thus, theoretical considerations, as well as *in vivo* strain and comparative morphometric data, can be invoked in support of the hypothesis that variation in primate mandibular corpus morphology reflects adaptation to variation in the amplitude and nature of strain associated with mastication of foods with different material properties. However, there are reasons for thinking that the influences on external mandible morphology of masticating foods of different material properties might be relatively minor. Although food-related differences in principal strain orientations on the lateral aspect of the corpus during mastication reported by Hylander (1979c: Table 10) are statistically significant, the differences are very small (<2°; Fig. 1), raising questions about their biological significance. Consider, for example, that the effects of chewing side on principal strain orientations are at least as large as, and usually larger than, effects of food type (average chew side difference = 26° in Table 8 of Hylander [1979c] and Hylander et al. [1987]). If large differences in strain regimes associated with chewing side demand trade-offs in mandibular corpus design, these might swamp effects on mandible morphology of smaller differences in strain regimes associated with chewing foods with different material properties.

Another issue, particularly relevant to this paper, is the fact that the majority of the variance in both the relative timing of jaw

Table 1
Terminology and abbreviations.

Term	Definition	Examples
Loading regime	Combination of external forces acting on the mandible	Muscle, joint, and bite forces
Deformation regime	Pattern of deformation associated with a loading regime	Bending, twisting
Stress regime	Pattern of internal forces at local points associated with a loading regime	Principal, shear, Von Mises stress
Strain regime	Pattern of strains (principal, shear, Von Mises) at local points associated with a loading regime	Principal, shear, Von Mises strain
FMP	Food material properties	

		Units
E	Young's modulus	MPa
R	Toughness	Jm^{-2}
ε_1	Maximum principal strain	Microstrain ($\mu\varepsilon$)
ε_2	Minimum principal strain	Microstrain ($\mu\varepsilon$)
γ_{max}	Shear strain	Microstrain ($\mu\varepsilon$)

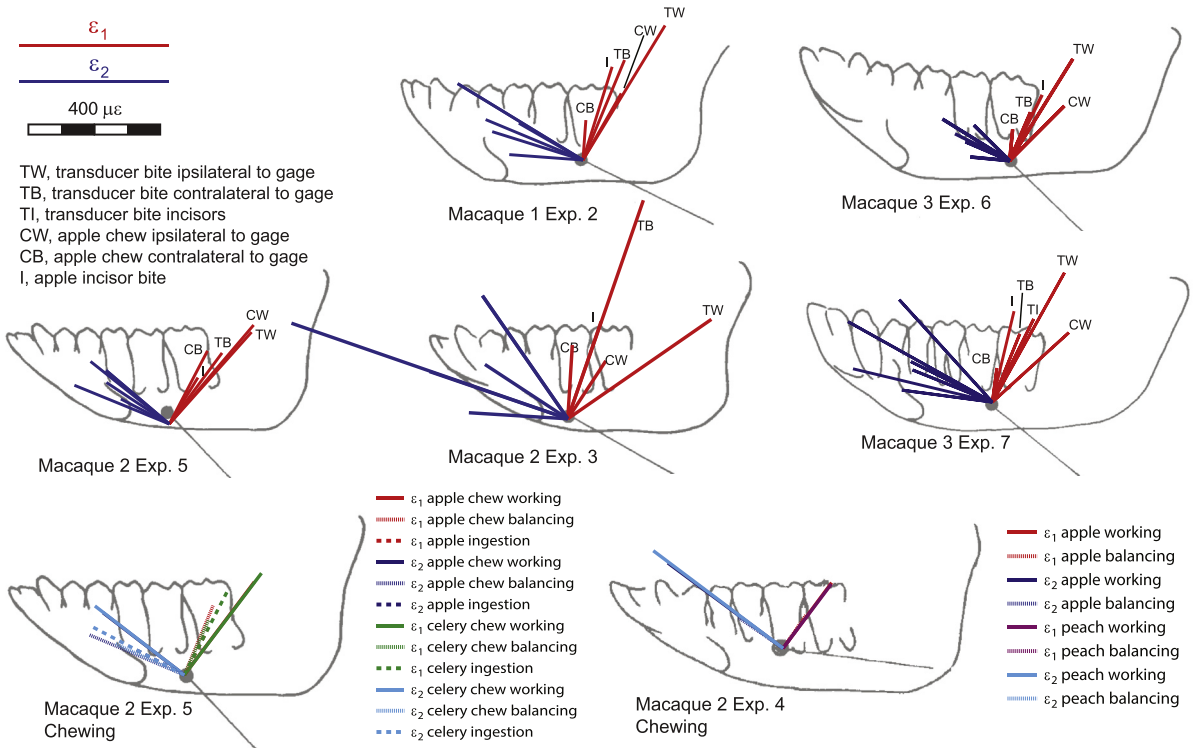

Figure 1. Diagrams of mean principal strain orientations and magnitudes recorded from the lateral aspect of the mandibular corpus of three *Macaca fascicularis* during transducer biting and apple ingestion and chewing, as reported by Hylander (1979a, b, c). Tracings of radiographs and orientations of reference elements are taken from Hylander (1979a, b, c: Fig. 8). Strain magnitude and orientation data are from Hylander (1979a, b, c: Tables 3 and 8).

muscle EMGs and jaw kinematics is found between gape cycles within feeding sequences, not between mastication sequences on different foods (Vinyard et al., 2008; Iriarte-Diaz et al., 2011). A feeding sequence begins when a food item is ingested and ends with the final swallow of that item. In experimental settings, when only one food item is ingested at a time, a large source of between-sequence variation in jaw muscle EMG activity and jaw kinematics is probably the different foods, which in the studies cited above included dried fruits, nuts, bamboo, leaves, and gelatin candies. However, there is also within-sequence variation in jaw muscle EMG and kinematics related to, and probably elicited by, variation in food bolus size and material properties resulting from intra-oral processing of the ingested food item, including food transport, fragmentation, and mixing with saliva (Hiiemae, 2000). The key point for the current paper is that jaw kinematics and jaw muscle EMG relative timing are important determinants of the loading, stress, strain, and deformation regimes in the mandibular corpus during feeding. Consequently, if jaw kinematics and EMG relative timing vary more within than between sequences, then mandibular corpus strain regimes probably also vary more within than between sequences. If mandibular corpus design has to accommodate not only variation in stress and strain regimes associated with chewing side, but also within-sequence variation associated with food processing, effects on mandibular corpus morphology of inter-sequence variation in the properties of foods being masticated may be insignificant or undetectable.

1.2. Is variation in mandibular corpus morphology related to variation in oral food processing behavior?

Primate mandibular corpus morphology has also been argued to vary between species that commonly employ different *oral food processing behaviors*. For example, Hylander (1979a) noted that mangabeys (*Lophocebus albigena*) have relatively deeper mandibular corpora than cercopithecines that spend less time using their incisors to bite hard fruits. He hypothesized that the relatively deeper mandibular corpora of mangabeys might have evolved to resist high sagittal bending moments associated with frequent incisor biting (Hylander, 1979a). Strain in the neck of the mandible varies between incision and mastication (Hylander and Bays, 1979; Hylander, 1979a), strain orientations on the labial surface of the symphysis vary widely with oral food processing behavior (Hylander, 1984), and strain orientations on the lateral aspect of the corpus during ingestion incision and isometric biting frequently differ from those recorded during mastication (Hylander, 1979c: Fig. 1). Thus, not only do mandibular corpus stress, strain, and deformation regimes differ significantly across oral food processing behaviors, but this variation appears larger than that experienced during mastication on different foods. If this is indeed the case, it suggests that inter-specific variation in mandibular corpus morphology might more directly reflect variation in the daily frequency and importance of different oral food processing behaviors (such as incisor biting versus premolar biting versus molar biting/mastication), rather than variation in the material properties of foods being chewed.

The relationships between variation in mandibular corpus morphology and variation in feeding behavior have been explored in a number of morphometric studies, with mixed results. Behavioral differences are argued to underlie differences in mandible shapes between gouging and non-gouging close-relatives (Vinyard et al., 2003; Vinyard and Ryan, 2006). Common marmosets (*Callithrix jacchus*) do not generate relatively high bite forces during tree gouging, predicting no significant differences in mandibular corpus morphology compared with *Saguinus* and *Saimiri*, a prediction confirmed by Vinyard and Ryan (2006). However, gouging primates do generate gouging forces at relatively wider jaw gapes, which in

C. jacchus is facilitated by lower condyle heights and longer jaw-muscle fiber lengths, a musculoskeletal configuration that allows common marmosets to operate over a more favorable portion of the length–tension curve at larger gapes (Vinyard et al., 2003; Eng et al., 2009; Taylor and Vinyard, 2009). In this case, inter-specific variance in feeding behavior (gape) exerts a strong influence on mandible morphology.

Daegling and McGraw (2001) compared mandibular corpus morphology in sympatric and similar-sized *Colobus polykomos* and *Procolobus badius*. *C. polykomos* not only consumes more seeds than *P. badius*, but it also harvests seeds from "thick woody pods of *Pentaclethera macrophylla*" and was predicted to have absolutely and relatively larger mandibular corpora (Daegling and McGraw, 2001). Not only were no differences found in symphyseal robusticity and corporal breadth at the M_2, but corpus height only distinguishes *C. polykomos* males from *P. badius* males; *C. polykomos* females are not distinct in corpus height. In a later study, Daegling and McGraw (2007) noted that *Lophocebus* employs incisor biting more frequently during hard object feeding than sympatric *Cercocebus*, predicting that *Lophocebus* would have a deeper symphysis and postcanine corpus and that *Cercocebus* would have a labiolingually thicker and larger symphysis and a larger postcanine corpus area to resist shearing forces. *Lophocebus* does have a deeper postcanine corpus, as predicted, but in contrast with predictions, the two species do not differ significantly in corpus cross-sectional area (at M_2), *Lophocebus* does not have a deeper symphysis, and the symphysis of *Cercocebus* is stronger in coronal bending than that of *Lophocebus* (Daegling and McGraw, 2007).

Taylor (2006b) compared the load resistance abilities of mandibles of *Pongo* species from Borneo—*Pongo pygmaeus wurmbii* and *Pongo pygmaeus morio*—with those of Sumatran Pongo—*Pongo pygmaeus abelii*. Both species of Bornean orangutans eat relatively tougher foods than *P. p. abelii*, using a range of behaviors, including powerful incision during ingestion and processing. Relative to *abelii*, both *morio* and *wurmbii* have deeper mandibular corpora and larger mandibular condyles relative to their incisor load arms, increasing their resistance to parasagittal bending and condylar compression during incision, but neither of the Bornean species has the broader mandibular corpus relative to *abelii* predicted for resisting torsional stresses generated during incision, and only *morio* has the deeper symphyseal shape predicted for resisting coronal bending of the symphysis during incision (Taylor, 2006b; Vogel et al., 2014). The significance of these results is constrained by the lack of detailed data on differences in feeding behaviors between the different species and subspecies of orangutans. However, it is noteworthy that deeper mandibular corpora relative to incisor load arms characterize both the hard object feeding orangutans and *Lophocebus*. This suggests that variation in the degree of powerful incisor biting might be a determinant of variation in mandibular corpus morphology.

The relationships between dietary toughness, feeding behavior, and mandible corpus morphology among *Cebus/Sapajus* species, the species studied for this paper, are also not clear-cut. *Sapajus* sp. is more durophagous than *Cebus capucinus*, employing their jaws in a range of extra-oral food processing and extraction behaviors. As predicted, *Sapajus apella* has improved jaw-muscle leverage (e.g., Cole, 1992; Wright, 2005a, b; Wright et al., 2009), and female *S. apella* have relatively more robust mandibular corpora than female *C. capucinus*, with more cortical bone in the cross-section (Daegling, 1992). However, male *apella* do not differ significantly from male *capucinus*, and although *Sapajus libidinosus* process and consume foods of exceptionally high toughness compared to *Cebus olivaceus* and *S. apella*, *S. libidinosus'* mandibular corpus shape does not significantly differ from that of *S. apella* (Wright, 2005a, b; Wright et al., 2009).

In this paper, we explore the relationships between feeding behaviors and patterns of strain in the mandibular corpus of *Sapajus* capuchin monkeys to better understand how mandible shape might be related to deformation and strain regimes during different behaviors. To evaluate the extent to which variation in food processing behavior is related to variation in mandibular strain regimes, we collected *in vivo* bone strain data from the mandibular corpora of three robust tufted capuchins (*Sapajus* sp.; Lynch-Alfaro et al., 2012; Wright et al., 2015) while they performed a wide range of food processing behaviors. The specific aims of this study were to test the following hypotheses: 1) variation in oral food processing behaviors, such as incisive and premolar biting and pulling, is associated with significant variation in strain regimes in the mandibular corpus, 2) mastication of foods with different material properties results in significant variation in strain regimes in the mandibular corpus, and 3) variation in strain regimes associated with different oral food processing behaviors is greater than variation in strain produced by mastication on foods of different material properties. The mandibular corpus was selected for study because it has been the focus of much of the prior work on mandibular biomechanics (Hylander, 1979b, 1988; Bouvier, 1986a, b; Daegling, 1989, 1990, 2007; Ravosa, 1991, 2000; Taylor, 2002, 2006b; Wallisch et al., 2009), because it is commonly preserved in the fossil record, and because it is easily accessed *in vivo*.

2. Materials and methods

2.1. Subjects

All procedures were approved by the University of Chicago IACUC. Three adult male *Sapajus sp.* served as subjects. The three individuals were robust, tufted capuchin monkeys, and can therefore be assigned to the genus *Sapajus* following Lynch-Alfaro et al. (2012) and Wright et al. (2015).[1] The subjects had all of their teeth and displayed no obvious asymmetries, diseases, or deformities of their feeding systems. At least three months prior to data recording, four Vitallium™ bone screws were implanted in their mandibles and four in their zygomatic arches. These percutaneous screws served as anchoring points for reflective markers used for recording of jaw kinematic data reported elsewhere (Reed and Ross, 2010; Iriarte-Diaz et al., 2011; Ross et al., 2012). In this study, kinematic data for two individuals were of high enough quality to be used to evaluate the effects of surgical strain gage placement on feeding behavior. It was not possible to rigorously compare jaw kinematics before and after screw placement. However, in the several months of data collection after placement of screws, the animals appeared to feed normally, including vigorous ingestion and mastication of a wide range of food items. They displayed no preferences for chewing side and their body weights were not affected by screw placement.

2.2. Strain-gage placement

During one experiment on each animal, three delta rosette strain gages (SA-06-030WY-120, Micromeasurements, Raleigh, NC) wired in a three-wire quarter-bridge circuit were attached to the mandibular corpus below M_2–M_3. Two gages were placed on the lateral surface and one gage on the medial surface (Fig. 2). The animals were food-deprived for 24 h before each experiment and then sedated with ketamine (4 mg/kg) and dexmedetomidine

[1] We do not have definitive DNA evidence or geographic locality of the individuals' ancestral populations and there is considerable within-species diversity in *Sapajus*. Thus, we do not assign the individuals to species.

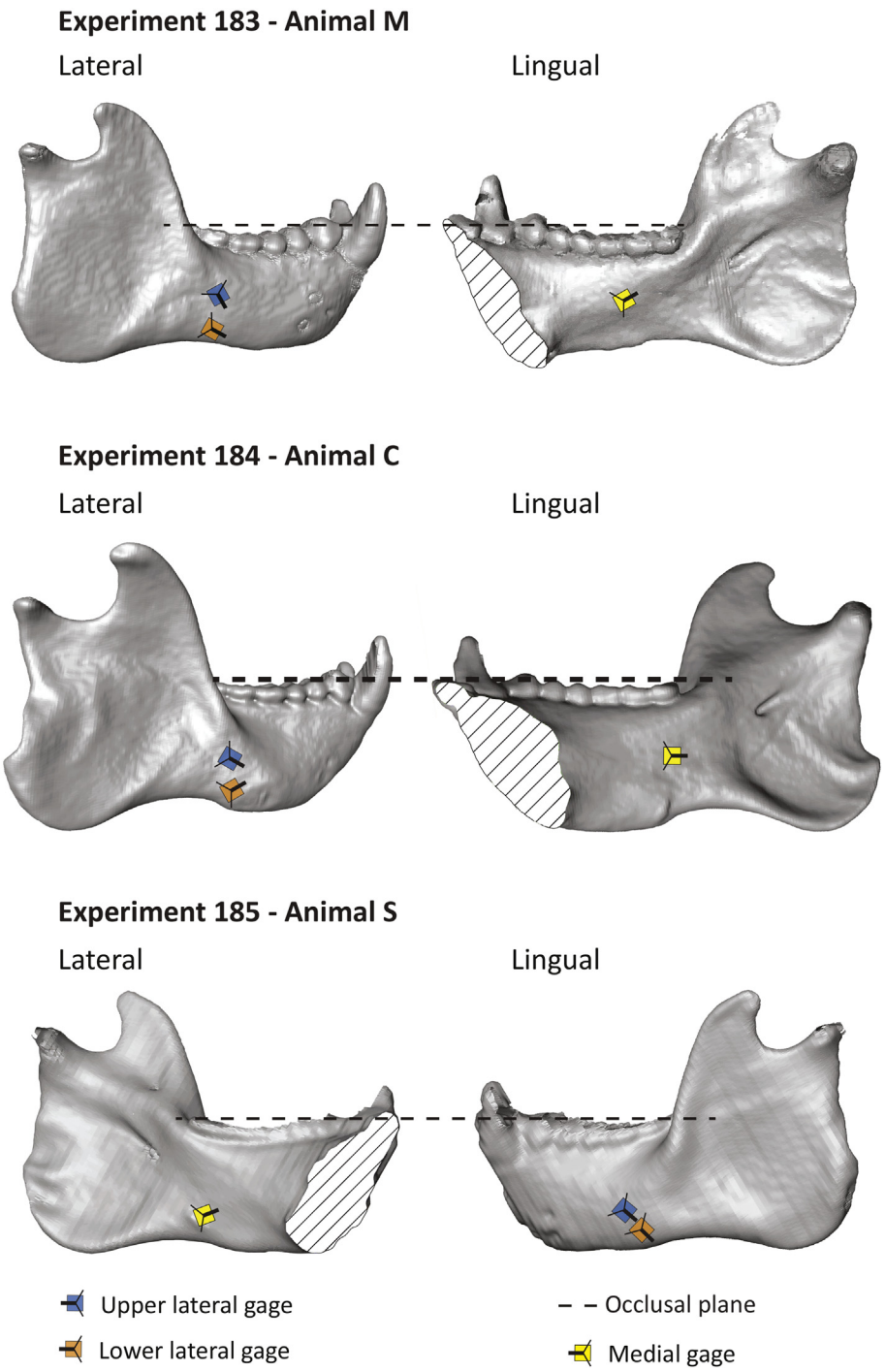

Figure 2. 3D surface renderings of CT scans of the mandibles of the three individuals used in this study showing locations, relative size, and orientations of the delta rosette strain gages. The lateral gages were placed 5 mm rostral to the insertion of the superficial masseter, one at mid-corpus height and one near the bottom edge of the corpus. This location corresponds to the lateral mandibular prominence in hominids where the root of the ramus merges with the corpus (Brown, 1997; Kimbel et al., 2004). The medial gage was placed inferior to the attachment of the mylohyoid muscle. Note that gages were placed on the right corpus during experiments 183 (animal M) and 184 (animal C), and on the left corpus in Experiment 185 (animal S). Gage positions and orientations relative to the occlusal plane were determined from radiographs taken following recording.

(150–200 μg/kg) prior to anesthesia with inhalant isofluorane delivered in O_2 (Theriault et al., 2008). After an adequate plane of anesthesia was achieved, a small incision was made in the skin overlying the inferior border of the corpus. Access to the lateral surface of the corpus required no disturbance of the masseter or buccinator muscles. The anterior digastric muscle in *Sapajus* has a large fleshy attachment to the medial surface of the corpus, extending posteriorly from the symphysis to the medial pterygoid attachment area and from the inferior edge of the corpus to the mylohyoid line. Consequently, access to the medial corpus gage site required detachment of a small portion of the anterior digastric from the corpus. As noted below, these procedures did not significantly impact jaw kinematics in the two animals in which this could be evaluated.

At each gage site, the periosteum was elevated to expose the cortical bone, a small area of the bone was degreased with clinical grade chloroform, and then the rosette was bonded to the bone with a cyanoacrylate adhesive. To prevent movements of the lead wires from causing strain in the gage circuit, the wires were bonded to the bone for 3–4 mm using the same adhesive. Following bonding of the strain gage and wires, the incision was sutured closed with the lead wires of the strain gage passing out through the incision. The wires were secured to the skin in areas where skin movement is minimal. Indwelling electromyography (EMG) electrodes were implanted in the anterior and posterior temporalis, superficial and deep masseter, and medial pterygoid muscles. Radiographs were taken to document strain gage position and orientation.

The animals were placed in a long-sleeved jacket and then secured in a commercially available restraint (XPL-517-CM, Plas Labs, Lansing, MI) that limited trunk movements while enabling the head and neck to move freely. The jacket sleeves were secured through pulleys to friction blocks that enabled the arms to be released to allow the animal to feed itself. The animals were allowed to recover for at least one hour after isofluorane anesthesia and at least two hours after ketamine sedation before data collection. Each of the three elements of the rosettes was connected to form one arm of a Wheatstone Bridge, with excitation at two volts. Voltage changes were conditioned and amplified on a Vishay 2310A system and then recorded using Vicon Motion analysis software. The animals were presented with a range of foods and bone strain, EMG, and jaw kinematic data were recorded while the animals ingested and chewed these foods. After each recording session (Experiment), the animal was again anesthetized, the gages were removed, the wound cleaned and closed with sutures, analgesics and antibiotics were administered, and the animal was returned to its cage. All animals recovered from all surgeries and recordings without complications.

2.3. Foods sampled

The animals were presented a variety of foods ranging in material and geometric properties in order to elicit the wide range of feeding behaviors observed during prior training sessions. The material properties of some of the foods presented to the animals were available in the literature and are presented in Table 2. These material properties were not used in statistical analyses and are only presented for qualitative comparisons by the reader. Though we lack data on the material properties of all the parts of all of the foods ingested and masticated, the data that we do have show a substantial range of material properties in both Young's modulus (ranging between 8.7 and 2978 MPa) and toughness (ranging between ~106 and 965 Jm^{-2}; Table 2). Geometric properties (size and shape) were not recorded for the food items; however, the food items were presented whole, including Brazil nuts, almonds, and walnuts in the shells. This represents a range of sizes, from the Brazil nuts and walnuts in shells to almonds. Not all animals ate all food types in all experiments, so Table 2 does not summarize the full range of material properties in all experiments. Moreover, the FMPs available to us (Table 2) are from the flesh on the inside of the nuts, not the shells on the outside.

2.4. Kinematic analysis

Rigid body kinematics of the jaws were calculated in Matlab using scripts from the KineMat toolbox (http://isbweb.org/software/movanal/kinemat/). To describe mandibular movement with respect to the fixed cranium, we used instantaneous helical angles, which are similar to Cardan/Euler angles that describe the rotation of a rigid body from one time step to the next (Woltring et al., 1985). Feeding sequences were divided into discrete feeding cycles (between consecutive maximum gapes). Gape cycles were standardized in two ways: first, timing was standardized by dividing each cycle into 100 time steps (percentages of the gape cycle); second, actual timing was maintained, but cycles were aligned so that maximum gape was centered at zero. For two of the individuals (C and S), it was possible to compare average kinematic values recorded prior to these strain gage experiments with values recorded during the experiments themselves.

2.5. Oral food processing behavior categories

Video recordings of the experiments were used to divide gape cycles into the following categories: incisor, canine, premolar, and molar ingestion bites; canine and incisor pulls; and mastication cycles. Biting side for incisor and premolar bites was determined from the videos; biting side for the mastication cycles was determined from analysis of the 3D jaw kinematics. Gape cycles in which the right molars were moving medially during the slow-close phase of the gape cycle were assigned to right chews; gape cycles in which the left molars were moving medially during the slow-close phase of the gape cycle were assigned to left chews.

Table 2
Foods used and material properties.

Food	Young's modulus, *E*, (MPa)	Fracture toughness, *R* (Jm^{-2})	Reference
	mean (SD)	mean (SD)	
Almond	19.42 (7.69)	308.6 (34.85)	Williams et al., 2005
Almond	21.6 (4.00)	245.8 (40.2)	Agrawal et al., 1997
Almond	8.7 (1.4)	105.7 (58.7)	Ross et al., 2009
Dried apricot	0.99 (0.29)	565.2 (102.93)	Williams et al., 2005
Dried apricot	5.9 (0.2)	830.0 (72.0)	Ross et al., 2009
Dried banana chip	NA	NA	
Brazil nut (seed)	33.84 (7.75)	160.8 (37.9)	Agrawal et al., 1997
Cashew nut	11.08 (2.28)	174.8 (44.4)	Agrawal et al., 1997
Coconut meat	NA	NA	
Dried dates	3.2 (0.48)	964.6 (114.31)	Agrawal et al., 2000
Hazelnut	12.2	166.2	Dominy, pers. comm.
Dried mango	NA	NA	
Pecan	NA	NA	
Popcorn kernel	325.4 (218.83)	2978.8 (678.34)	Williams et al., 2005

NA = not available.

2.6. Strain analysis

The strain data were sampled at a rate of ≥1000 Hz, then converted to microstrain (με, 1×10^{-6}) using calibration files made during the recording sessions. Sequences were selected for analysis on the basis of the quality of the strain data and were rejected if there was obvious movement artifact. All gape cycles in a sequence were included except those where the magnitude of the strains decreased so as to be unreliably distinguishable from noise (which ranged from 5 to 10 mV in each channel).

Strain (ε), measured in με, is a dimensionless unit equaling the change in length of an object divided by its original length. The maximum principal strain (ε_1) is usually the largest tensile strain value, while the minimum principal strain is usually the largest compressive strain value (ε_2). The maximum shear strain (γ-max) is equal to ε_1 minus ε_2. Selected feeding sequences were analyzed using custom written software in IGOR Pro (Versions 4.0 and 6.43a). Specifically, the direction of ε_1 relative to the A-element of the gage, the magnitude of the shear strains, and the ratio of maximum to minimum strains ($|\varepsilon_1/\varepsilon_2|$) were calculated with standard equations. The magnitude and timing of the peak shear strains were calculated for each power stroke, then the direction of the maximum principal strain and the ratio of maximum to minimum strains at the same point in time were calculated.

The orientations and magnitudes of ε_1 and ε_2 strain "vectors" recorded at the time of peak strain were plotted and visualized prior to analysis (Supplementary Online Material [SOM] Figures S1eS3). (Although strain is not strictly speaking a vector, the orientation and magnitude of the principal strains can be visualized as such.) These plots facilitate estimation of relative magnitudes of peak tensile and compressive strains, as well as an appreciation of the range of strain orientations recorded and the relationships between strain orientations and strain magnitudes. The strain vector plots were created by converting strain orientations (in degrees) and magnitudes (in με) to polar coordinates. The orientations of the vectors relative to the mandibles were determined from notes and radiographs taken during the surgeries, using the postcanine tooth row as the reference plane. In lateral radiographs, this plane was defined as a line from the most posterior point on the occlusal surface of the lower third molar (M_3) to the paraconid of the first lower premolar (P_2).

Data from three gages placed around the circumference of the mandible allow calculation of the normal strain distribution across the section of the gages. From this distribution, maximum and minimum normal strains for the cross section and the orientation of the neutral axis within the cross section were then calculated using a custom macro for Igor Pro modified from one provided by B. Demes, Stony Brook University (Rybicki et al., 1977; Demes, 1998, 2007; Demes et al., 2001). The orientation of the neutral axis provides one measure of the strain and deformation regimes during feeding. To calculate the orientation of the neutral axis of bending, normal strains (strains normal to the plane of the cross section) were calculated from peak principal strains recorded during each bite. Cross-sectional geometry of the mandible was determined from CT scans (1 mm slice thickness) of the specimens. Normal strains were calculated assuming that material properties are homogeneous through the cross section.

Data analyses were performed in Matlab (R2012B), IBM SPSS Statistics (Version 22), Igor Pro 4.0 (Lake Oswego, OR), and Oriana 2.02e (Kovach Computing Services, www.kovcomp.com). Circular statistics were calculated for the orientations of ε_1 at each gage site, with chew cycles grouped according to cycle type (incisor biting, premolar biting, mastication) and biting side (i.e., whether the animal bit ipsilateral or contralateral to the gage site, yielding "working-side" and "balancing-side" chews, respectively). Descriptive statistics presented are: the angle (μ) of the mean vector relative to the tooth row; the length of the mean vector (r), ranging from 0 to 1, with a larger r value indicating the observations are clustered more closely around the mean; the concentration (κ), the maximum likelihood estimate of the population concentration (Fisher, 1993; Mardia and Jupp, 2000) (a parameter specific to the von Mises distribution that measures the departure of the distribution from a uniform distribution, when $\kappa = 0$ the distribution is uniform, with higher values converging on a normal distribution); the circular variance $V = 1 - r$; the circular standard deviation $S = (-2\ln(r))^{1/2}$ (in radians); the standard error of the mean (formula 4.42 in Fisher, 1993); and the weighted mean vector, which is the mean orientation of ε_1 weighted by the magnitude of ε_1. Note that the length of the mean vector is not an estimate of the mean magnitude of ε_1, but instead an estimate of the degree to which the ε_1 orientations cluster. We used Rayleigh's test of uniformity to determine whether all strain orientations are equally likely. A significant Rayleigh's test indicates that strain or neutral axis orientations are significantly non-uniform; i.e., there is a predominant orientation. Watson's U^2 Test is used to determine whether the data are derived from a von Mises distribution and, hence, whether parametric tests of strain orientations were appropriate.

To test the third hypothesis—that variation in strain regimes is higher across different behaviors than across chews on different foods—at each gage site in each experiment the variation in ε_1 orientation was quantified across all non-chew cycle types, all chews (including left and right chews), and for left and right chews separately using S, the range of mean ε_1 orientation, and the range of weighted mean ε_1 orientation. The ranges of means were calculated by computing the differences between the highest and lowest mean values of ε_1 orientations across behaviors, across chews on different foods, and within and across chewing sides. These values were then tabulated for comparison. Variation in neutral axis orientation was assessed using S and the range of mean orientation. (Weighted means cannot be calculated for neutral axis orientation.)

Methods for fully nested hierarchical analyses of variance for angular data are not currently available. Instead, two-way ANOVAs of angular data were performed using the Circular Statistics Toolbox in Matlab 2012b to test for effects of food and behavior on orientations of principal strain and neutral axes of bending. Games and Howell post-hoc tests were performed. Balancing side chews (contralateral to gages) and working side chews (ipsilateral to gages) were tested separately. Because these failed distributional assumptions required for parametric tests, mean ε_1 and neutral axis orientations recorded during different behaviors and during eating of different foods were compared using a nonparametric Mardia-Watson-Wheeler test. The effects of food type and chewing side on mean ε_1 magnitude and $\log_{10} |\varepsilon_1/\varepsilon_2|$ ratios during chewing cycles were tested using a parametric two-way ANOVA with side as a fixed effect, food type as a random effect, and chew number as a covariate. Grape and date chewing were excluded because the strain magnitudes were too low to be reliable. The effects on ε_1 magnitudes of cycle type, food type, and cycle number in the sequence were evaluated using a parametric two-way ANOVA, with cycle type and food as random effects and cycle number as a covariate.

3. Results

To evaluate whether gage placement affected feeding kinematics, we compared the jaw kinematics for two subjects (C and S) recorded during these strain gage experiments with kinematics recorded in previous experiments when no gages were placed. For experimental subject C, we found no clear differences in the mean angular velocity of the mandible (Fig. 3A, B). Kinematic patterns of

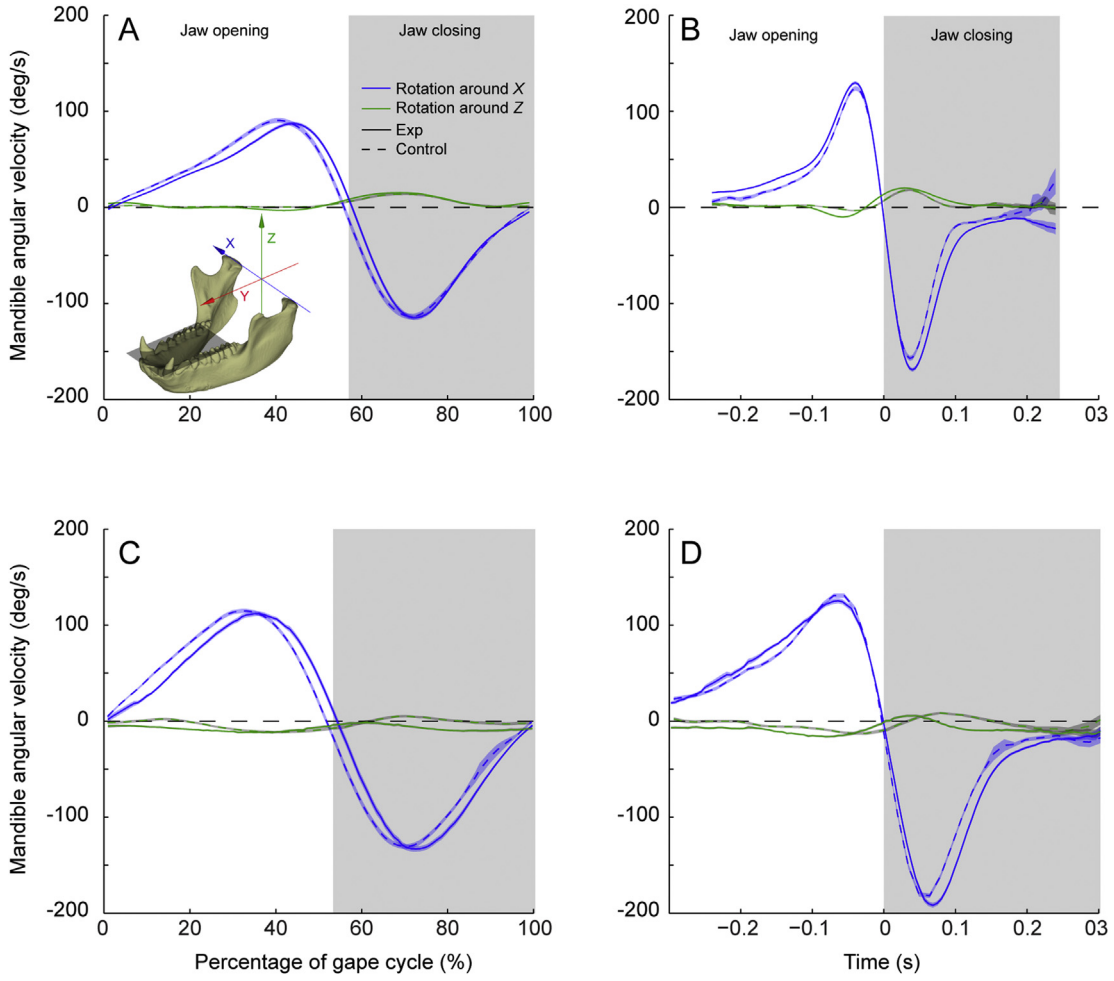

Figure 3. Average mandible kinematics through a gape cycle comparing control (no gages, dashed lines) and experimental (with gages, solid lines) conditions for two of the experimental subjects. Plots indicate the angular velocity of the mandible with respect to the fixed cranium. Blue traces show the rotation around the X-axis (see inset), indicating jaw opening and closing (positive values for jaw opening and negative values for jaw closing), while green traces show the rotation around the Z-axis, indicating lateral deviation (positive for a mandible moving towards the working side and negative for a mandible moving towards the balancing side). Top panels show the mandible kinematics of experimental subject C for a time-standardized gape cycle (A) and in absolute time, centered around maximum gape (B). Bottom panels show the mandible kinematics of experimental subject S for a time-standardized gape cycle (C) and in absolute time, centered around maximum gape (D). Kinematic traces are presented as mean values and their respective standard errors of the mean (lines and shadow traces around them, respectively). Gray sections indicate the jaw-closing phase of the gape cycle. (For interpretation of the references to color in this figure legend, the reader is referred to the web version of this article.)

jaw opening/closing and lateral displacements were qualitatively similar, reaching comparable peak points and points of inflection (i.e., changes in angular velocity) at similar times between data collected with the strain gages (n = 1318 gape cycles) and that collected without gages (n = 828 gape cycles). For experimental subject S, we also found similar kinematic patterns between experiments when gages where present (n = 747 gape cycles) and when absent (n = 1067 gape cycles; Fig. 3C, D). Slight differences in the timing of peak angular velocity of the mandible around the Z-axis (i.e., lateral mandible rotation) were found between experiments (Fig. 3D), but otherwise the same kinematic pattern is observed.

Strain orientations and magnitudes are presented for Experiment 183 in Figures 4–6, for Experiment 184 in Figures 7–9, and for Experiment 185 in Figure 10. SOM Figures S1–3 present all the strain vectors for ε_1 and ε_2 recorded during these experiments. The ε_1 magnitude data are summarized in Figure 11. The ε_1 data for Experiment 183 are presented in Tables 3 and 4, for Experiment 184 in Tables 5 and 6, and for Experiment 185 in Table 7. ANOVA results for strain magnitudes and ratios are given in Tables 8 and 9. Ranges of circular standard deviations, means, and weighted means are given in Table 10.

4. Experiment 183

In Experiment 183, animal M ate almonds, banana chips, cashews, dates, and hazelnuts, while strain data were recorded from the right corpus. The available data on Young's modulus (E) of these foods range from 3.2 to 12 MPa and on fracture toughness (R) range from 105 to 965 Jm^{-2} (Table 2). Strain orientations during date chews were excluded from the analyses summarized below because the strain magnitudes were so low that they approached the level of noise in each element of the rosette strain gage (ca. 5–10 με; Table 4).

4.1. Oral food processing behaviors

During oral processing behaviors, all strain orientations were not equally likely (Rayleigh's test, Table 3). Oral food processing behavior had a significant effect on ε_1 orientation at all three gage

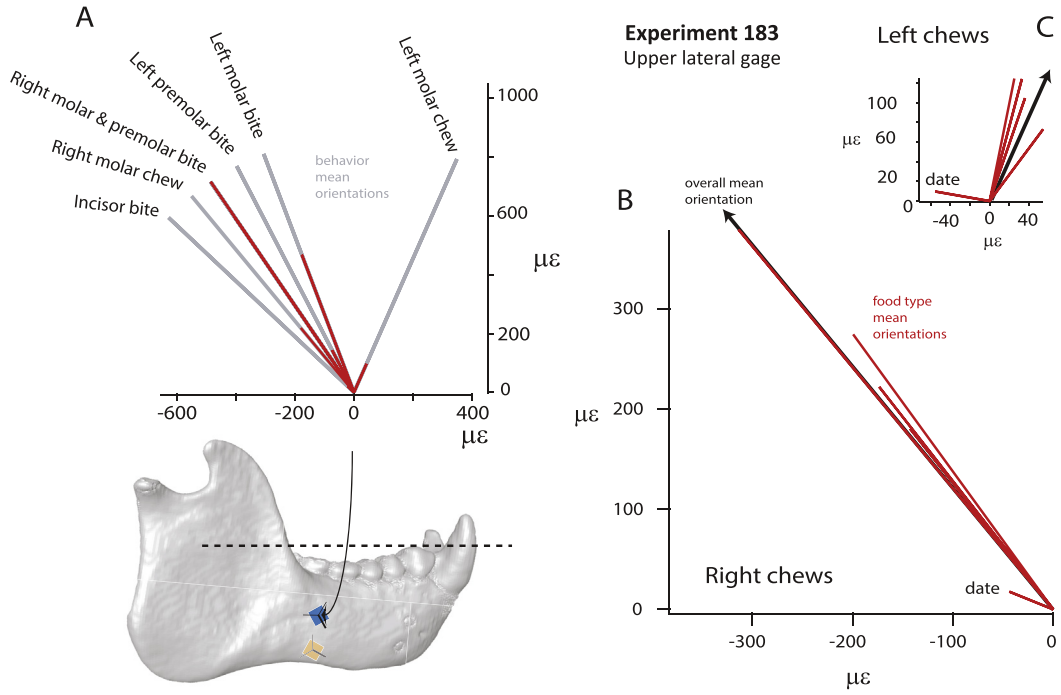

Figure 4. Mean ε_1 orientation and magnitude recorded from the upper lateral gage during feeding by animal M in Experiment 183. Red lines are vectors illustrating orientation and magnitude of ε_1. A) Mean ε_1 orientations recorded during different behaviors. Gray lines in A illustrate mean orientations where low magnitudes make it difficult to distinguish the vectors. B) Mean ε_1 orientations during left (balancing side) chews, with each vector representing a different food type. C) Mean ε_1 orientations during right (working side) chews, with each vector representing a different food type. Black arrows illustrate mean ε_1 orientations during all left chews (B) and all right chews (C). (For interpretation of the references to color in this figure legend, the reader is referred to the web version of this article.)

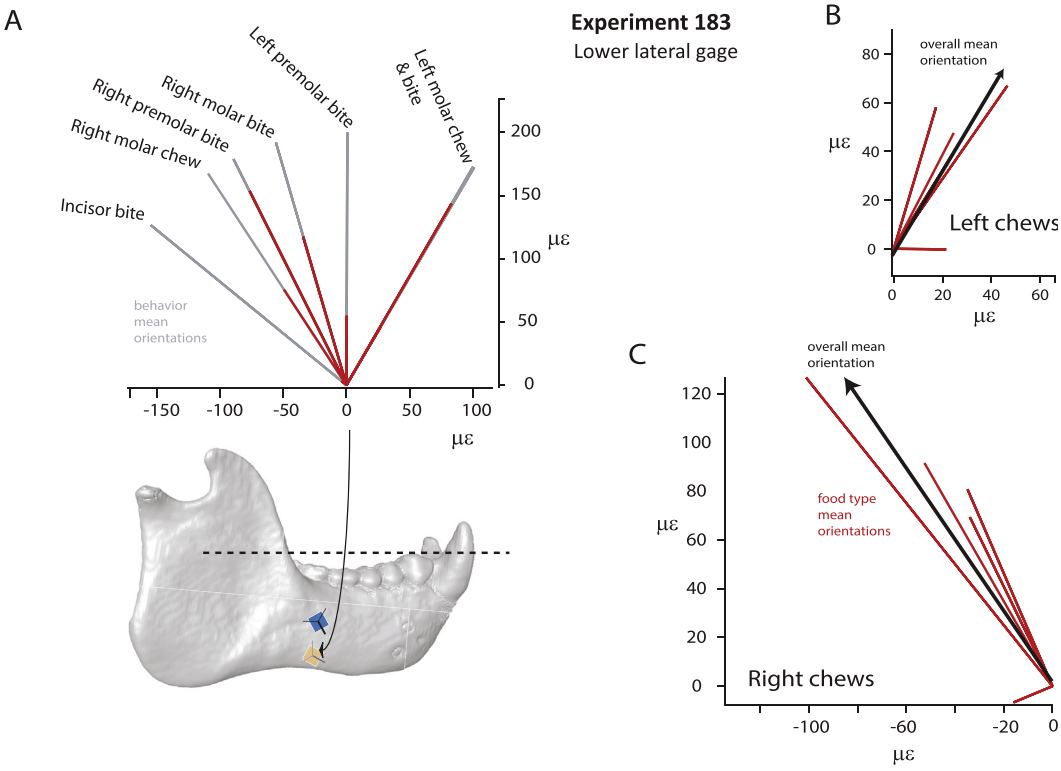

Figure 5. Mean ε_1 orientation and magnitude recorded from the lower lateral gage during feeding by animal M in Experiment 183. Red lines are vectors illustrating orientation and magnitude of ε_1. A) Mean ε_1 orientations recorded during different behaviors. Gray lines in A illustrate mean orientations where low magnitudes make it difficult to distinguish the vectors. B) Mean ε_1 orientations during left (balancing side) chews, with each vector representing a different food type. C) Mean ε_1 orientations during right (working side) chews, with each vector representing a different food type. Black arrows illustrate mean ε_1 orientations during all left chews (B) and all right chews (C). (For interpretation of the references to color in this figure legend, the reader is referred to the web version of this article.)

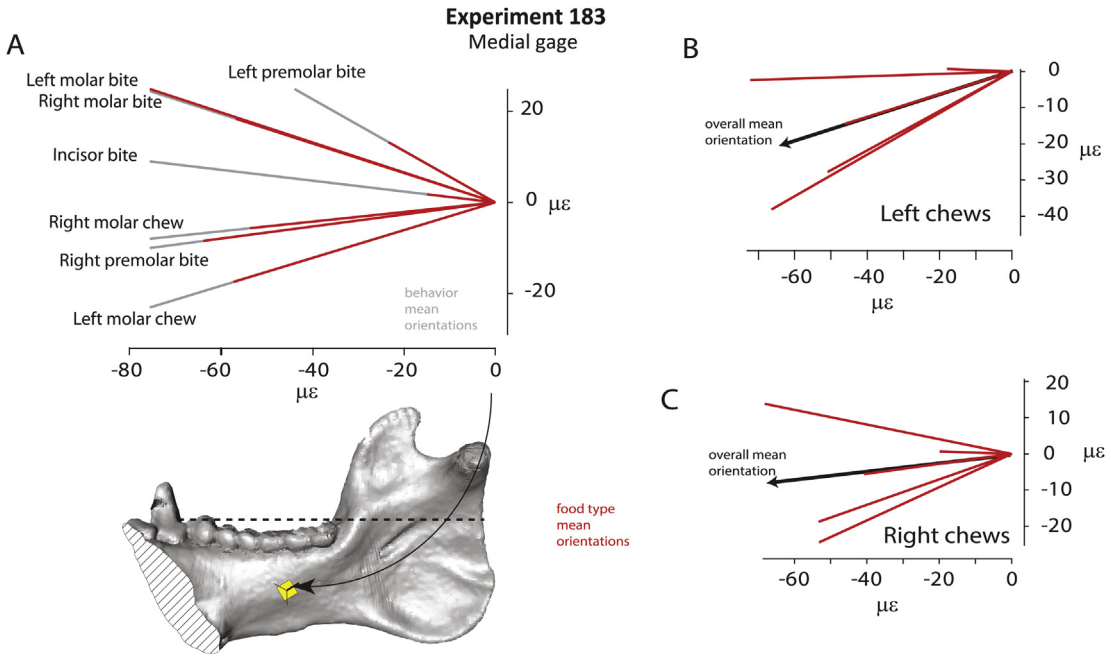

Figure 6. Mean ε_1 orientation and magnitude recorded from the medial gage during feeding by animal M in Experiment 183. Red lines are vectors illustrating orientation and magnitude of ε_1. A) Mean ε_1 orientations recorded during different behaviors. Gray lines in A illustrate mean orientations where low magnitudes make it difficult to distinguish the vectors. B) Mean ε_1 orientations during left (balancing side) chews, with each vector representing a different food type. C) Mean ε_1 orientations during right (working side) chews, with each vector representing a different food type. Black arrows illustrate mean ε_1 orientations during all left chews (B) and all right chews (C). (For interpretation of the references to color in this figure legend, the reader is referred to the web version of this article.)

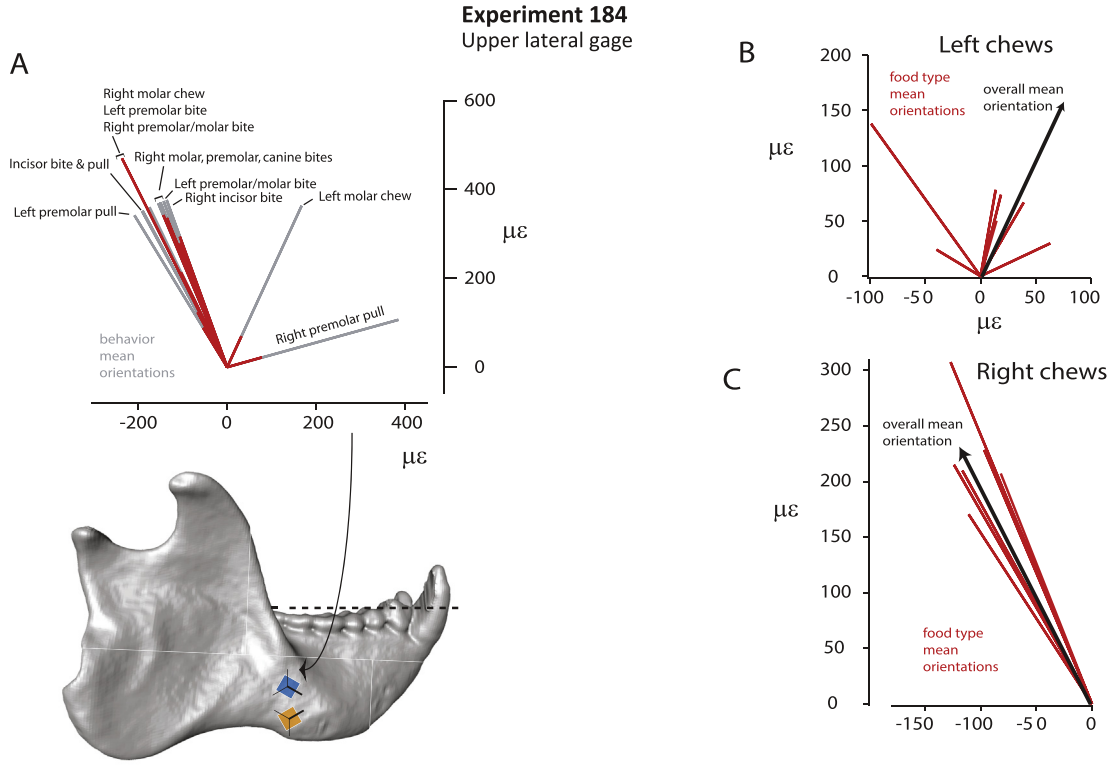

Figure 7. Mean ε_1 orientation and magnitude recorded from the upper lateral gage during feeding by animal C in Experiment 184. Red lines are vectors illustrating orientation and magnitude of ε_1. A) Mean ε_1 orientations recorded during different behaviors. Gray lines in A illustrate mean orientations where low magnitudes make it difficult to distinguish the vectors. B) Mean ε_1 orientations during left (balancing side) chews, with each vector representing a different food type. C) Mean ε_1 orientations during right (working side) chews, with each vector representing a different food type. Black arrows illustrate mean ε_1 orientations during all left chews (B) and all right chews (C). (For interpretation of the references to color in this figure legend, the reader is referred to the web version of this article.)

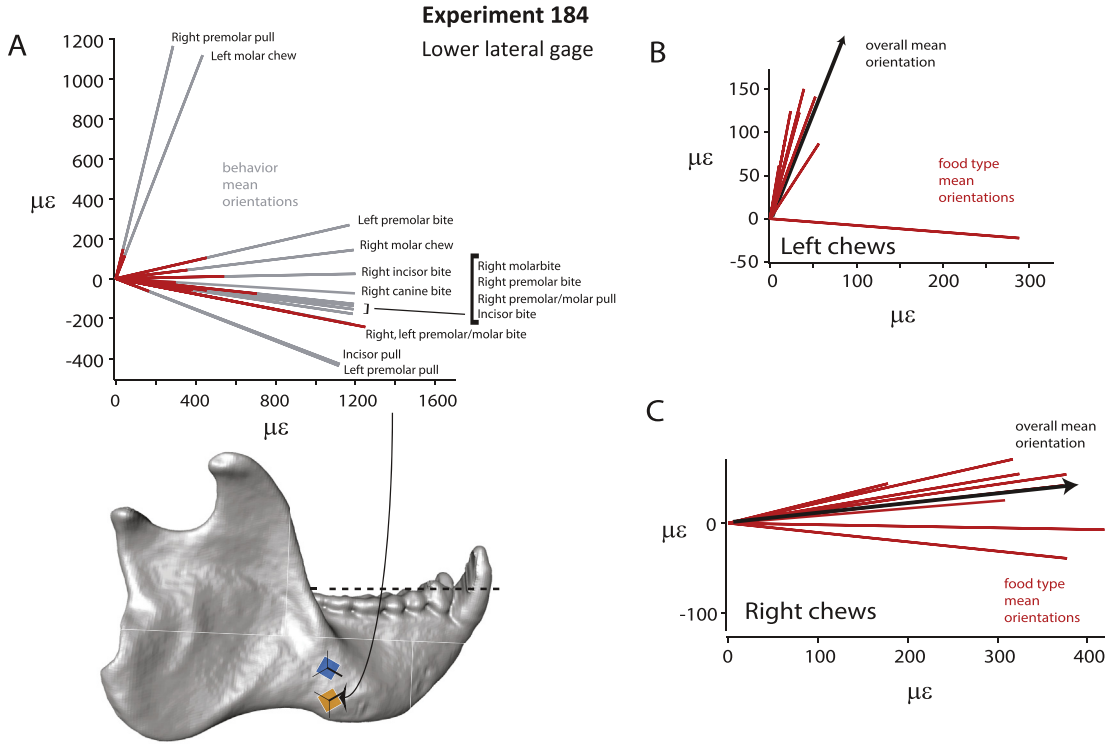

Figure 8. Mean ε_1 orientation and magnitude recorded from the lower lateral gage during feeding by animal C in Experiment 184. Red lines are vectors illustrating orientation and magnitude of ε_1. A) Mean ε_1 orientations recorded during different behaviors. Gray lines in A illustrate mean orientations where low magnitudes make it difficult to distinguish the vectors. B) Mean ε_1 orientations during left (balancing side) chews, with each vector representing a different food type. C) Mean ε_1 orientations during right (working side) chews, with each vector representing a different food type. Black arrows illustrate mean ε_1 orientations during all left chews (B) and all right chews (C). (For interpretation of the references to color in this figure legend, the reader is referred to the web version of this article.)

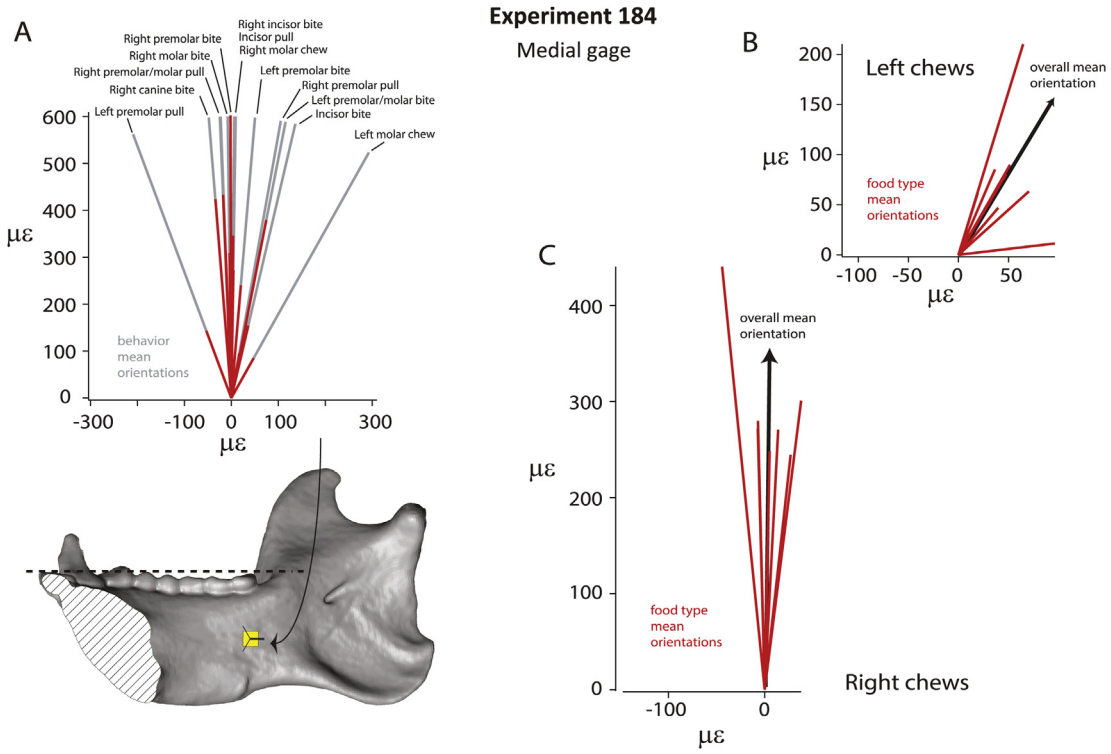

Figure 9. Mean ε_1 orientation and magnitude recorded from the medial gage during feeding by animal C in Experiment 184. Red lines are vectors illustrating orientation and magnitude of ε_1. A) Mean ε_1 orientations recorded during different behaviors. Gray lines in A illustrate mean orientations where low magnitudes make it difficult to distinguish the vectors. B) Mean ε_1 orientations during left (balancing side) chews, with each vector representing a different food type. C) Mean ε_1 orientations during right (working side) chews, with each vector representing a different food type. Black arrows illustrate mean ε_1 orientations during all left chews (B) and all right chews (C). (For interpretation of the references to color in this figure legend, the reader is referred to the web version of this article.)

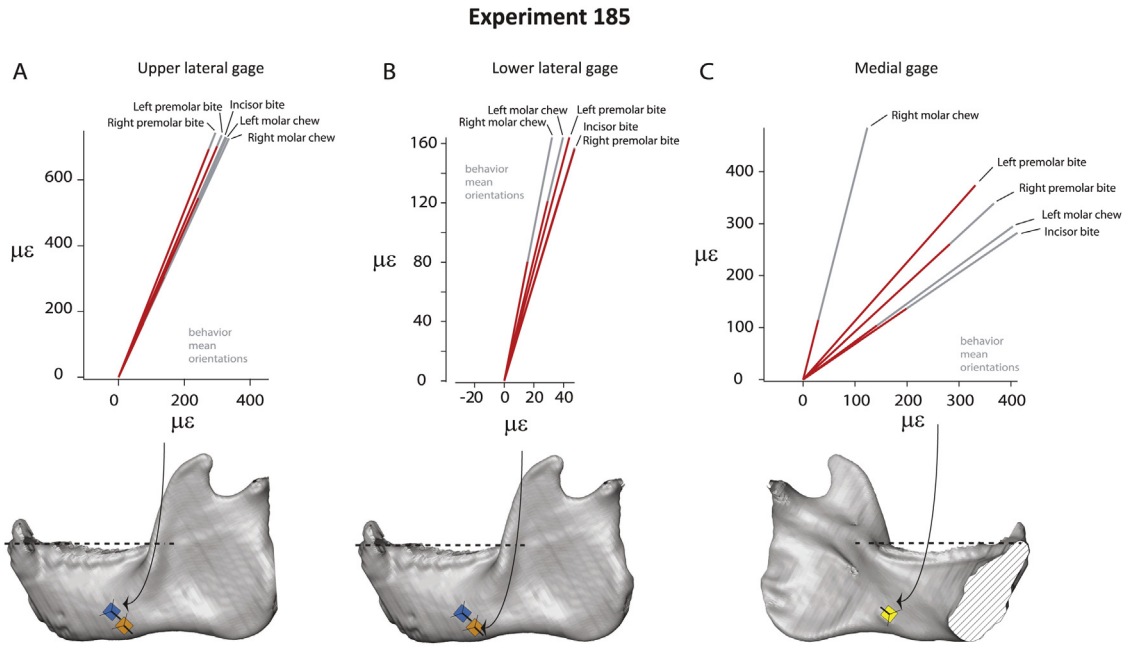

Figure 10. Mean ε_1 orientation and magnitude recorded during feeding by animal S in Experiment 185. Red lines are vectors illustrating orientation and magnitude of ε_1. Gray lines illustrate mean orientations where low magnitudes make it difficult to distinguish the vectors. A) Mean ε_1 orientations recorded from the upper lateral gage during different behaviors. B) Mean ε_1 orientations recorded from the lower lateral gage during different behaviors. C) Mean ε_1 orientations recorded from the medial gage during different behaviors. (For interpretation of the references to color in this figure legend, the reader is referred to the web version of this article.)

sites, as well as on neutral axis orientation (upper lateral, $F = 69.5$; lower lateral, $F = 147.4$; medial, $F = 17.02$; neutral axis, $F = 18.0$; all $p < 0.001$). Strain magnitudes varied across oral processing behaviors and were always higher (mean and maximum) at the upper corpus than the lower corpus site (compare values for upper lateral and lower lateral in Table 3). Mean strain magnitudes ranged from 30 to 866 με at the upper lateral corpus site, from 5 to 172 με at the lower lateral corpus site, and from 15 to 80 με at the medial corpus site (Table 3). The highest ε_1 magnitude recorded was 2138 με, recorded from the upper lateral gage site during isometric biting on the contralateral molars (Table 3). The highest strain magnitudes at all gage sites were recorded during biting, not chewing.

The effects of cycle type, cycle number, and food type on ε_1 magnitude and $|\varepsilon_1/\varepsilon_2|$ ratios were evaluated using two-way ANOVAs, with cycle type and food as random effects and cycle number as a covariate (Table 8a). At all gage sites, cycle number had the strongest effect (i.e., highest F-values) on ε_1 magnitude, and at both lateral gage sites cycle type had the next strongest effect. Food type only had a significant effect at the medial gage site. At the two lateral gage sites, cycle type × food interaction effects were significant.

The most consistent effect on $|\varepsilon_1/\varepsilon_2|$ ratios across all gage sites was the interaction effect between cycle type and food type: i.e., the way that cycle type impacts $|\varepsilon_1/\varepsilon_2|$ ratios varies with food type. At the upper lateral gage site, $|\varepsilon_1/\varepsilon_2|$ ratios were significantly impacted by cycle type and by the interaction between cycle type and food type, but neither food type nor cycle number was significant. At the lower lateral gage site, $|\varepsilon_1/\varepsilon_2|$ ratios were significantly impacted by all main and interaction effects, but food type and interaction effects were the weakest. At the medial gage site, $|\varepsilon_1/\varepsilon_2|$ ratios were significantly impacted by cycle number, food type, and cycle type × food interactions, but not cycle type.

4.2. Chewing

During chewing, all strain orientations were not equally likely (Rayleigh's test, Table 4). ANOVA for circular data revealed variable effects of food type on mandibular corpus principal strain and neutral axis orientation during chewing cycles. During right chews, food type had a significant effect on mean ε_1 orientation at the medial ($F = 41.1$, $p < 0.001$) and lower lateral gage sites ($F = 3.03$, $p = 0.03$), but not at the upper lateral gage site. Food type affected neutral axis orientation during right chews ($F = 3.5$, $p = 0.02$). During left chews, food type had a significant effect on mean ε_1 orientation at the medial ($F = 8.2$, $p < 0.001$) and upper lateral gage sites ($F = 11.5$, $p < 0.001$), but not at the lower lateral gage site. Food type also affected neutral axis orientation during left chews ($F = 9.5$, $p < 0.001$).

Strain magnitudes varied during chewing on different foods and were always higher at the upper corpus (compare upper lateral and lower lateral strain data in Table 4) and usually higher during chewing ipsilateral to the gage (i.e., on the right side). The lowest mean strain magnitudes were associated with chewing dates (18 με), and the highest mean strain magnitudes were associated with chewing on banana chips (128 με; Table 4). Maximum strain magnitudes ranged between 46 με (dates) and 1065 με (banana chips).

To evaluate the effects of food type and chew side during chew cycles on ε_1 magnitude and $|\varepsilon_1/\varepsilon_2|$ ratios, we used two-way ANOVAs with food as a random effect, chew side as a fixed effect, and cycle number as a covariate (Table 8b). During chewing cycles, ε_1 magnitudes were significantly affected by cycle number at all gage sites and by chew side at the lateral gage sites. Food type did not have a significant effect on ε_1 magnitude at any gage site, but there were significant interaction effects between chew side and food type. The most consistent effect on $|\varepsilon_1/\varepsilon_2|$ ratios across all gage sites was the interaction effect between chew side and food type: the way that food type impacts $|\varepsilon_1/\varepsilon_2|$ ratios varies with chew side. $|\varepsilon_1/\varepsilon_2|$ ratios are not affected by food type during chewing at lateral gage sites, but they are at medial gage sites.

4.3. Chewing versus non-chewing oral behaviors

Table 10 compares S (circular standard deviation) and ranges of means and weighted means of ε_1 orientations across all non-chewing oral food processing behaviors, across all chews, and across left and

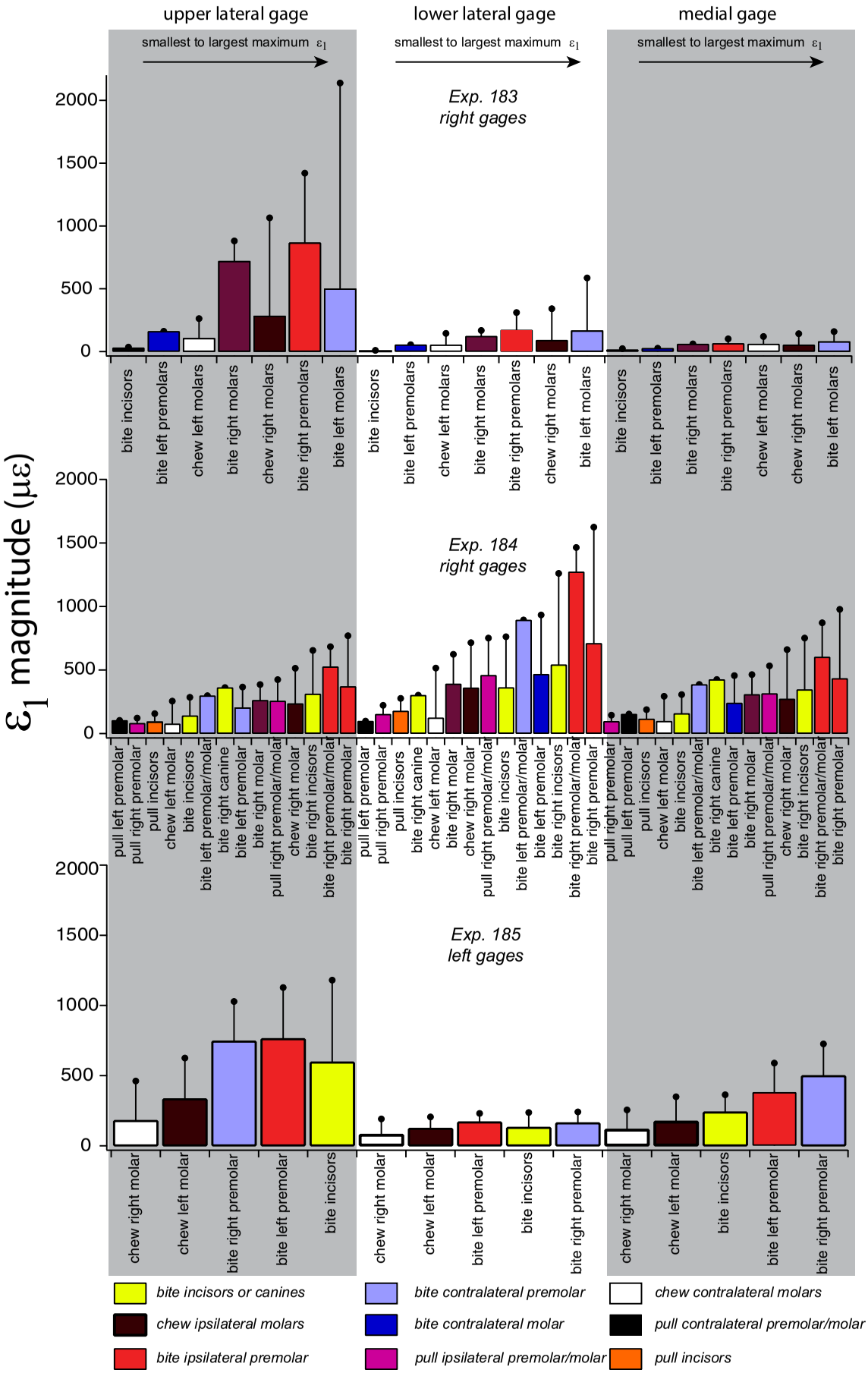

Figure 11. Mean (box) and maximum (whisker) ε_1 strain magnitudes recorded during the three experiments, separated by behavior. Strains varied by behavior, with the largest strains at all gage sites being during biting and not during chewing.

Table 3
Experiment 183 data by behavior.

Gage site	Upper lateral						
Behavior	Chew	Isometric bite	Isometric bite	Isometric bite	Isometric bite	Isometric bite	Chew
Bite point	Left (contralateral) molars	Left (contralateral) molars	Left (contralateral) premolars	Incisors	Right (ipsilateral) premolars	Right (ipsilateral) molars	Right (ipsilateral) molars
n	139	22	1	4	3	2	179
Mean Vector (μ)	245.1	287.8	297.4	223.4	304.2	304.3	304.4
Length of Mean Vector (r)	0.875	0.936	1	0.166	0.999	1	0.864
Weighted Mean Vector (WMV)	253.0	294.9	297.4	212.1	303.6	304.3	307.0
Length of WMV (in variable units)	94.981	489.361	161.316	5.517	865.833	719.24	278.196
Length of WMV (r, scaled 0–1)	0.362	0.229	1	0.156	0.61	0.817	0.261
ε_1 magnitude mean	105.869	499.911	161.316	30.134	866.246	719.24	283.671
ε_1 magnitude standard deviation	49.678	4.53E+02		5.54E+00	576.988	228.202	1.76E+02
ε_1 magnitude maximum	262.206	2137.92	161.316	35.434	1420.37	880.603	1064.89
Concentration	4.302	8.068		0	173.007	6.80E+06	3.997
Circular Standard Deviation	29.61	20.87		108.61	2.25	0.01	30.92
Rayleigh Test (Z)	106.415	19.268	1	0.11	2.995	2	133.766
Rayleigh Test (*p*)	<1E-12	1.10E-08	0.512	0.907	0.034	0.137	<1E-12
Rao's Spacing Test (U)	250.371	283.967		150.554			307.74
Rao's Spacing Test (*p*)	<0.01	<0.01		0.50 > p > 0.10			<0.01
Watson's U^2 Test (von Mises, U^2)	0.48	0.247					8.091
Watson's U^2 Test (*p*)	<0.005	<0.005					<0.005
Gage site	Lower lateral						
Behavior	Chew	Isometric bite	Isometric bite	Isometric bite	Isometric bite	Isometric bite	Chew
Bite point	Left (contralateral) molars	Left (contralateral) molars	Left (contralateral) premolars	Incisors	Right (ipsilateral) premolars	Right (ipsilateral) molars	Right (ipsilateral) molars
n	139	22	1	4	3	2	179
Mean Vector (μ)	239.6	239.9	269.8	320.7	296.5	286.2	303.2
Length of Mean Vector (r)	0.752	0.422	1	0.561	0.994	0.996	0.898
Weighted Mean Vector (WMV)	65.9	44.8	89.8	3.9	116.0	108.1	119.1
Length of WMV (in variable units)	43.261	57.383	54.856	1.815	171.018	122.114	88.531
Length of WMV (r, scaled 0–1)	0.299	0.098	1	0.196	0.551	0.729	0.26
ε_1 magnitude mean	54.043	166.154	54.856	5.169	171.66	122.554	90.472
ε_1 magnitude standard deviation	27.807	120.415		3.357	124.045	6.36E+01	55.625
ε_1 magnitude maximum	144.896	585.971	54.856	9.278	310.387	167.52	340.935
Concentration	2.38	0.93		0.991	22.361	12.095	5.199
Circular Standard Deviation	43.25	75.28		61.61	6.28	5.22	26.56
Rayleigh Test (Z)	78.629	3.915	1	1.259	2.964	1.983	144.381
Rayleigh Test (*p*)	<1E-12	0.018	0.512	0.304	0.035	0.14	<1E-12
Rao's Spacing Test (U)	259.14	253.785		158.748			299.121
Rao's Spacing Test (*p*)	<0.01	<0.01		0.50 > p > 0.10			<0.01
Watson's U^2 Test (von Mises, U^2)	1.513	0.381					4.726
Watson's U^2 Test (*p*)	<0.005	<0.005					<0.005
Gage site	Medial						
Behavior	Chew	Isometric bite	Isometric bite	Isometric bite	Isometric bite	Isometric bite	Chew
Bite point	Left (contralateral) molars	Left (contralateral) molars	Left (contralateral) premolars	Incisors	Right (ipsilateral) premolars	Right (ipsilateral) molars	Right (ipsilateral) molars
n	139	22	1	4	3	2	179
Mean Vector (μ)	196.9	161.8	150.5	173.2	187.5	162.1	186.0
Length of Mean Vector (r)	0.92	0.932	1	0.999	0.992	0.973	0.935
Weighted Mean Vector (WMV)	201.0	164.6	150.5	174.2	187.2	162.4	183.4
Length of WMV (in variable units)	55.115	76.449	26.856	14.98	64.162	58.226	50.112
Length of WMV (r, scaled 0–1)	0.462	0.482	1	0.633	0.634	0.951	0.353
ε_1 magnitude mean	60.008	79.761	26.856	15.007	64.642	59.819	54.152
ε_1 magnitude standard deviation	3.00E+01	39.116		6.225	3.38E+01	1.95	30.924
ε_1 magnitude maximum	119.368	158.693	26.856	23.674	101.227	61.198	141.903
Concentration	6.558	7.652		138.236	16.261	1.903	8.002
Circular Standard Deviation	23.35	21.47		3.07	7.37	13.32	20.96
Rayleigh Test (Z)	117.735	19.118	1	3.989	2.951	1.895	156.582
Rayleigh Test (*p*)	<1E-12	1.21E-08	0.512	0.007	0.036	0.158	<1E-12
Rao's Spacing Test (U)	271.528	263.648		261.711			275.832
Rao's Spacing Test (*p*)	<0.01	<0.01		<0.01			<0.01
Watson's U^2 Test (von Mises, U^2)	0.741	0.18					0.228
Watson's U^2 Test (*p*)	<0.005	<0.01					<0.005

(*continued on next page*)

Table 3 (*continued*)

Gage site	Neutral axis						
Behavior	Chew	Isometric bite	Isometric bite	Isometric bite	Isometric bite	Isometric bite	Chew
Bite point	Left (contralateral) molars	Left (contralateral) molars	Left (contralateral) premolars	Incisors		Right (ipsilateral) molars	Right (ipsilateral) molars
n	139	22	1	4	3	2	179
Mean Vector (μ)	32.9	−3.9	6.5	22.8	25.8	22.8	24.0
Length of Mean Vector (r)	0.888	0.893	1	0.987	1	1	0.983
Concentration	4.763	4.949		15.909		661.556	29.13
Circular Standard Deviation	27.92	27.32		9.11	3263.3	0.70	10.71
Rayleigh Test (Z)	109.62	17.527	1	3.9	0.52	2	172.854
Rayleigh Test (*p*)	<1E-12	3.31E-08	0.512	0.009	3	0.137	<1E-12
Rao's Spacing Test (U)	258.447	249.006		246.527	0.033		302.229
Rao's Spacing Test (*p*)	<0.01	<0.01		<0.01			<0.01
Watson's U^2 Test (von Mises, U^2)	0.947	0.062					1.269
Watson's U^2 Test (*p*)	<0.005	0.5 > p > 0.25					<0.005

right chews separately. In Experiment 183, at the upper lateral gage site, S in ε_1 orientations was highest across all chew cycles (working and balancing sides pooled) and next highest across all non-chewing behaviors; at the lower lateral gage site, S was highest across all non-chew cycles and next highest across all chews; at the medial gage site, ε_1 orientation S was highest across all chews because of the wide range across contralateral chews (i.e., on the balancing side) and the next highest range was across ipsilateral chews; and in the neutral axis orientation, S was highest on the balancing side and next highest across all non-chew cycles. Comparing ranges of means of ε_1 orientations reveals that at the lateral gage sites, the highest ranges are seen across all chews, whereas the second highest ranges are seen across all non-chew behaviors, while the reverse is true at the medial gage site and for the neutral axis. When ranges of weighted mean ε_1 orientations are compared in Experiment 183, the widest ranges are seen across all chews, whereas the second widest are seen across all non-chew behaviors.

5. Experiment 184

In this experiment, the animal ate walnuts, Brazil nuts, pecans, hazelnuts, almonds, popcorn, mango, apricot, and coconut, while strain data were recorded from the right corpus. The available data on values of *E* for these foods range from 0.99 to 325 MPa and values of *R* range from 105 to 2979 Jm^{-2}.

5.1. Oral food processing behaviors

During oral processing behaviors, all strain orientations were not equally likely (Rayleigh's test, Table 5). Oral food processing behavior had a significant effect on ε_1 orientation at all gage sites, but not on neutral axis orientation (upper lateral, $F = 104.6$; lower lateral, $F = 40.8$; medial, $F = 12.1$; all $p < 0.001$).

Strain magnitudes varied across oral processing behaviors and were always higher (both mean and maximum) at the lower lateral gage site (Table 5). Mean strain magnitudes ranged between 77 and 526 με at the upper lateral corpus, 98–1273 με at the lower lateral corpus, and 96–603 με at the medial corpus gage site. The highest mean and maximum strains were always associated with biting on the working-side "premolars/molars."

The effects on ε_1 magnitude and $|\varepsilon_1/\varepsilon_2|$ ratios of cycle type, cycle number in the sequence, and food type were evaluated using two-way ANOVAs (cycle type and food, random effects), with cycle number as a covariate (Table 8a). As in Experiment 183, in Experiment 184 cycle number had the strongest (or nearly the strongest) effect on ε_1 magnitude at all gage sites. Cycle type had the next strongest effect at all gage sites. Food type had a significant effect at all gage sites in Experiment 184, but in all cases the F-values are relatively low. Cycle type × food interaction effects were significant at all gage sites.

As in Experiment 183, the most consistent effect on $|\varepsilon_1/\varepsilon_2|$ ratios across all gage sites in Experiment 184 was the interaction effect between cycle type and food type: the way that cycle type impacts $|\varepsilon_1/\varepsilon_2|$ ratios varies with food type. At the lower lateral gage site, only cycle number and cycle type × food interactions had significant effects on $|\varepsilon_1/\varepsilon_2|$ ratios. At the medial gage site, cycle number and cycle type × food interactions had significant effects on $|\varepsilon_1/\varepsilon_2|$ ratios: food type was not significant.

5.2. Chewing

During chewing, all strain orientations were not equally likely (Rayleigh's test, Table 6). During left chews (gages on balancing side), food type had a significant effect on mean ε_1 orientation at the medial ($F = 4.11$; $p < 0.001$) and upper lateral gage sites ($F = 11.3$; $p < 0.001$), but not at the lower lateral gage site, nor on neutral axis orientation. During right chews (gages on working side), food type did not have a significant effect on mean ε_1 orientation at any of the corpus gage sites. A parametric two-way ANOVA of $\log_{10} |\varepsilon_1/\varepsilon_2|$ ratios revealed that at the upper gage site both chew side and food type were significant ($F = 16.1$ $p < 0.001$; $F = 8.0$, $p = 0.004$, respectively), but interaction effects were not. At the lower lateral gage site, neither food type nor chew side effects were significant. At the medial gage site, interaction effects ($F = 5.8$, $p < 0.001$) and chew side ($F = 7.7$, $p = 0.02$) were significant, but food type was not.

Strain magnitudes varied with FMP and foods being chewed, with mean strain magnitudes ranging between 41 με (walnut, upper lateral corpus, left chew side) and 419 με (almond, lower lateral corpus, right chew side), with maximum strains as high as 715 με (Brazil nut, lower lateral corpus, right chews). The highest maximum strains occur during popcorn chewing at the upper lateral corpus (both right and left chews), the lower lateral corpus (left chews), and the medial corpus (right and left chews). For most foods, there is considerable overlap in mean strains during chewing (relatively high standard deviations); mean chew strains associated with popcorn, our most mechanically challenging food, stand out as usually exhibiting the least amount of overlap with mean chew strains associated with other foods (Table 6).

The effects on ε_1 magnitude and $|\varepsilon_1/\varepsilon_2|$ ratios of food type and chew side during chew cycles were assessed using two-way ANOVAs with food as a random effect, chew side as a fixed effect, and cycle number as a covariate (Table 8b). As in Experiment 183, in Experiment 184, ε_1 magnitudes at the upper lateral gage site were

Table 4
Experiment 183 chewing data by food.

Gage site	Upper lateral right									
Chew side	Left chews					Right chews				
Food	Almond	Banana chip	Cashew	Hazelnut	Date	Almond	Banana chip	Cashew	Hazelnut	Date
n	34	13	43	37	12	57	16	33	54	19
Mean Vector (μ)	253.975	254.126	232.281	257.934	201.001	127.975	129.658	128.423	126.04	187.555
Length of Mean Vector (r)	0.913	0.92	0.96	0.929	0.625	0.994	0.996	0.998	1	0.525
Weighted Mean Vector (WMV)	259.765	261.813	235.603	259.768	248.704	127.045	130.357	127.646	126.226	217.983
Length of WMV (in variable units)	101.025	121.665	87.704	116.955	27.788	281.125	491.824	229.924	339.378	16.942
Length of WMV (r, scaled 0–1)	0.385	0.575	0.582	0.544	0.185	0.465	0.462	0.61	0.531	0.114
ε_1 magnitude mean	110.574	128.42	90.97	127.05	56.191	281.962	492.317	230.123	339.497	47.437
ε_1 magnitude standard deviation	54.781	68.103	34.894	38.807	39.787	135.137	276.133	90.732	139.622	34.229
ε_1 magnitude maximum	262.206	211.654	150.705	214.82	150.393	604.505	1064.89	376.846	639.353	148.712
Concentration	6.055	5.087	12.628	7.329	1.51	85.413	128.663	308.859	1108.021	1.228
Circular Standard Deviation	24.396	23.448	16.464	21.975	55.595	6.218	5.061	3.263	1.722	65.028
Rayleigh Test (Z)	28.362	10.995	39.592	31.939	4.68	56.333	15.876	32.893	53.951	5.24
Rayleigh Test (*p*)	3.90E-12	7.96E-07	<1E-12	<1E-12	0.007	<1E-12	2.08E-07	<1E-12	<1E-12	0.004
Rao's Spacing Test (U)	261.2	245.158	286.222	272.203	234.635	317.746	314.043	331.201	341.794	239.053
Rao's Spacing Test (*p*)	<0.01	<0.01	<0.01	<0.01	<0.01	<0.01	<0.01	<0.01	<0.01	<0.01
Watson's U^2 Test (von Mises, U^2)	0.317	0.03	0.451	0.119	0.16	0.753	0.276	0.29	0.184	0.224
Watson's U^2 Test (*p*)	<0.005	>0.5	<0.005	<0.05	<0.005	<0.005	<0.005	<0.005	<0.005	<0.005

Gage site	Lower lateral right									
Chew side	Left chews					Right chews				
Food	Almond	Banana chip	Cashew	Hazelnut	Date	Almond	Banana chip	Cashew	Hazelnut	Date
n	34	13	43	37	12	57	16	33	54	19
Mean Vector (μ)	253.428	235.153	238.212	242.654	179.282	113.289	128.598	116.022	119.853	202.799
Length of Mean Vector (r)	0.978	0.627	0.921	0.55	0.706	0.99	0.997	0.996	0.999	0.833
Weighted Mean Vector (WMV)	254.844	247.771	241.494	245.084	170.447	112.85	127.58	115.525	120.026	184.967
Length of WMV (in variable units)	59.185	62.878	46.405	31.761	14.557	87.523	161.771	76.887	105.516	12.668
Length of WMV (r, scaled 0–1)	0.5	0.434	0.529	0.267	0.314	0.451	0.474	0.615	0.527	0.276
ε_1 magnitude mean	60.563	81.492	50.155	53.501	21.446	88.049	162.184	77.149	105.626	17.421
ε_1 magnitude standard deviation	23.829	50.377	20.075	20.127	11.098	44.245	86.57	29.804	42.617	9.898
ε_1 magnitude maximum	118.447	144.896	87.663	118.851	46.322	194.022	340.935	125.042	200.379	45.891
Concentration	23.045	1.528	6.647	1.32	1.565	48.244	146.18	129.262	469.863	3.334
Circular Standard Deviation	12.069	55.403	23.176	62.641	47.77	8.292	4.747	5.049	2.645	34.628
Rayleigh Test (Z)	32.524	5.103	36.51	11.197	5.988	55.818	15.891	32.745	53.885	13.186
Rayleigh Test (*p*)	<1E-12	0.004	<1E-12	5.95E-06	0.001	<1E-12	2.07E-07	<1E-12	<1E-12	4.09E-07
Rao's Spacing Test (U)	307.805	226.276	270.904	285.173	247.738	322.27	319.603	329.457	338.968	273.725
Rao's Spacing Test (*p*)	<0.01	<0.01	<0.01	<0.01	<0.01	<0.01	<0.01	<0.01	<0.01	<0.01
Watson's U^2 Test (von Mises, U^2)	0.155	0.178	0.429	0.593	0.176	0.181	0.047	0.034	0.05	0.304
Watson's U^2 Test (*p*)	<0.025	<0.005	<0.005	<0.005	<0.005	<0.01	>0.5	>0.5	0.5 > p > 0.25	<0.005

Gage site	Medial right									
Chew side	Left chews					Right chews				
Food	Almond	Banana chip	Cashew	Hazelnut	Date	Almond	Banana chip	Cashew	Hazelnut	Date
n	34	13	43	37	12	57	16	33	54	19
Mean Vector (μ)	181.895	208.613	197.442	209.846	177.897	168.53	204.711	187.86	199.403	178.108
Length of Mean Vector (r)	0.827	0.984	0.969	0.978	0.999	0.921	0.981	0.981	0.977	1
Weighted Mean Vector (WMV)	184.507	211.707	201.733	211.198	177.835	165.548	200.824	188.213	198.451	178.499
Length of WMV (in variable units)	59.564	57.748	47.17	75.659	17.965	64.629	57.048	40.507	55.312	19.876
Length of WMV (r, scaled 0–1)	0.509	0.591	0.538	0.634	0.512	0.481	0.402	0.49	0.616	0.551
ε_1 magnitude mean	72.274	58.014	48.409	76.548	17.978	69.586	58.545	41.175	56.546	19.887
ε_1 magnitude standard deviation	27.903	31.616	23.156	24.108	9.52	39.48	28.964	16.353	18.443	9.732
ε_1 magnitude maximum	116.932	97.646	87.625	119.368	35.063	134.337	141.903	82.629	89.798	36.072
Concentration	3.234	25.165	16.239	22.519	477.197	6.598	26.05	26.102	22.211	1071.34
Circular Standard Deviation	35.321	10.18	14.448	12.213	2.295	23.269	11.337	11.325	12.299	1.751
Rayleigh Test (Z)	23.25	12.596	40.351	35.357	11.981	48.333	15.386	31.735	51.568	18.982
Rayleigh Test (*p*)	2.09E-10	1.33E-06	<1E-12	<1E-12	1.74E-06	<1E-12	2.68E-07	<1E-12	<1E-12	1.97E-08
Rao's Spacing Test (U)	225.784	298.627	304.522	291.262	322.288	266.669	300.494	306.945	308.356	335.769
Rao's Spacing Test (*p*)	<0.01	<0.01	<0.01	<0.01	<0.01	<0.01	<0.01	<0.01	<0.01	<0.01
Watson's U^2 Test (von Mises, U^2)	0.068	0.201	0.431	0.362	0.036	0.174	0.112	0.354	0.035	0.22
Watson's U^2 Test (*p*)	0.25 > p > 0.15	<0.005	<0.005	<0.005	>0.5	<0.01	0.1 > p > 0.05	<0.005	>0.5	<0.005

(*continued on next page*)

Table 4 (*continued*)

Gage site	Neutral axis									
Chew side	Left chews					Right chews				
Food	Almond	Banana chip	Cashew	Hazelnut	Date	Almond	Banana chip	Cashew	Hazelnut	Date
n	34	13	43	37	12	57	16	33	54	19
Mean Vector (μ)	41.245	25.923	28.635	30.614	39.348	17.501	29.911	24.516	23.678	39.42
Length of Mean Vector (r)	0.888	0.741	0.931	0.923	0.839	0.988	0.998	0.996	0.999	0.941
Concentration	4.753	1.79	7.479	6.746	2.623	42.989	259.061	122.311	468.071	8.785
Circular Standard Deviation	27.952	44.375	21.737	22.989	34.003	8.79	3.563	5.191	2.65	19.937
Rayleigh Test (Z)	26.799	7.136	37.236	31.498	8.438	55.674	15.938	32.73	53.885	16.833
Rayleigh Test (*p*)	1.37E-11	2.72E-04	<1E-12	<1E-12	1.93E-05	<1E-12	2.01E-07	<1E-12	<1E-12	7.50E-08
Rao's Spacing Test (U)	258.166	201.374	279.375	261.765	248.736	314.161	326.433	328.234	341.828	254.922
Rao's Spacing Test (*p*)	<0.01	<0.01	<0.01	<0.01	<0.01	<0.01	<0.01	<0.01	<0.01	<0.01
Watson's U^2 Test (von Mises, U^2)	0.201	0.108	1.016	0.887	0.11	0.073	0.106	0.275	0.147	0.051
Watson's U^2 Test (*p*)	<0.005	<0.05	<0.005	<0.005	<0.05	0.25 > p > 0.15	0.1 > p > 0.05	<0.005	<0.025	0.5 > p > 0.25

significantly affected by chew side and cycle number. However, unlike Experiment 183, food type did have a significant effect on ε_1 magnitudes at the upper lateral gage site, but chew side × food type interaction effects were not significant. At the lower lateral gage site, chew side, cycle number, and chew side × cycle number interactions had significant effects on ε_1 magnitudes. Food type was not significant. At the medial gage site, chew side, cycle number, and food type had significant effects on ε_1 magnitudes, but interaction effects between chew side and food type were not significant. As in Experiment 183, the most consistent effect on $|\varepsilon_1/\varepsilon_2|$ ratios across all gage sites was the interaction effect between chew side and food type: the way that food type impacts $|\varepsilon_1/\varepsilon_2|$ ratios varies with chew side. At all three gage sites, $|\varepsilon_1/\varepsilon_2|$ ratios are not affected by food type during chewing and this ratio is also not impacted by chew side at lateral gage sites.

5.3. Chewing versus non-chewing oral behaviors

Table 10 compares S and ranges of means and weighted means of ε_1 orientations across all non-chewing oral food processing behaviors, across all chews, and across left and right chews separately. At the upper lateral gage site, ε_1 orientation S was highest across all chew cycles (working and balancing sides pooled) and second highest across all non-chews. At the lower lateral gage site, ε_1 orientation S was highest across all non-chew cycles and second highest across all chews. At the medial gage site, ε_1 orientation S was highest across all chews because of the high value of S across contralateral chews (i.e., on the balancing side), and second highest during ipsilateral chews. S in neutral axis orientation was highest on the balancing side and second highest across all chews. The widest range of means at the lateral gage site was across all chews, driven by the wide range across balancing side chews, and the second highest range was across all non-chew behaviors. At the lower lateral gage site, the widest range was across all non-chew behaviors and the second widest range was across all chews. At the medial gage site and the neutral axis, the widest range in mean orientations was across all chews, with the second largest being across left chews. The widest range of weighted means was across all chews (and balancing side chews) at the two lateral gage sites, with the second highest ranges being across all non-chew behaviors. At the medial gage site, the widest range in weighted means was across all chews and the second highest across all left chews.

6. Experiment 185

During this experiment, the animal only chose to eat Brazil nuts, so the effects of food type on ε_1 orientation during mastication were not assessed. Strains were recorded from the left corpus.

6.1. Oral food processing behaviors and chews

During oral processing behaviors, all strain orientations were not equally likely (Rayleigh's test, Table 7). ANOVA for circular data using cycle type as a factor revealed cycle type to have a significant effect on ε_1 orientation at the medial gage site only ($F = 17.8$; $p < 0.001$). One-way ANOVA revealed a significant effect of cycle type on $\log_{10}$ $|\varepsilon_1/\varepsilon_2|$ ratios at all three gage sites (upper lateral, $F = 7.1$, $p < 0.001$; lower lateral $F = 15.3$, $p < 0.001$; medial, $F = 9.8$, $p < 0.001$).

Strain magnitudes vary across oral processing behaviors with average strains ranging between 180 and 763 με (upper lateral corpus), 82–170 με (lower lateral corpus), and 118–499 με (medial corpus). Strains are always highest at the upper lateral corpus. At medial and lower lateral corpus gage sites, the highest strain magnitudes (both mean and maximum) are associated with premolar biting. At the upper lateral corpus gage site, the highest strain magnitudes were recorded during incisor biting (Table 7).

The range of mean values for ε_1 orientation across oral food processing behaviors was 3.1° at the upper lateral gage site, 5.8° at the lower lateral gage site, and 41.3° at the medial gage site (Fig. 10). Mean neutral axis orientation across behaviors only varied by 12°.

7. Discussion

The data presented here provide insight into variation in mandibular corpus strain regimes—ε_1 orientation and magnitude, the ratio of $|\varepsilon_1/\varepsilon_2|$, the orientation of the neutral axis of bending—during a wide range of oral food processing behaviors on a wide range of foods. Although Young's modulus and toughness data are available for some parts of some of these foods (Table 2), material properties data are not available for the intact Brazil nut, walnut, and almond shells that the animals broke open during premolar and molar biting. Thus, the FMP ranges presented in Table 2 might under-estimate the range of FMPs presented to the

Table 5
Experiment 184 data by behavior.

Gage site	Upper lateral													
Behavior	Bite	Chew	Chew	Bite	Bite	Pull	Bite	Bite	Bite	Pull	Pull	Pull	Bite	Bite
Bite point	Right premolar	Left molar	Right molar	Left premolar	Incisors	Incisors	Right incisors	Left premolar/molar	Right premolar/molar	Left premolar	Right premolar/molar	Right premolar	Right molar	Right canine
n	31	259	356	12	30	13	4	1	3	1	2	2	4	1
Mean Vector (μ)	292.799	245.2	295.795	296.398	298.444	298.64	289.927	290.858	296.669	301.41	292.432	195.44	292.304	291.984
Length of Mean Vector (r)	0.998	0.657	0.885	0.678	0.617	0.97	0.999	1	0.999	1	1	0.178	1	1
Weighted Mean Vector (WMV)	292.285	249.965	291.563	293.213	292.94	296.539	291.44	290.858	296.11	301.41	291.989	305.563	292.348	291.984
Length of WMV (in variable units)	370.538	39.914	231.14	176.875	120.07	90.988	311.882	297.702	525.393	103.593	256.607	42.116	261.905	361.708
Length of WMV (r, scaled 0–1)	0.481	0.156	0.45	0.484	0.421	0.581	0.477	1	0.768	1	0.604	0.347	0.679	1
ε_1 magnitude mean	370.778	76.629	235.984	204.118	140.354	93.323	312.238	297.702	525.982	103.593	256.618	81.172	261.962	361.708
ε_1 magnitude standard deviation	192.901	46.39	112.685	100.241	91.212	37.163	228.593		138.212		237.514	56.838	95.773	
ε_1 magnitude maximum	769.914	255.587	513.726	365.634	285.393	156.715	654.14	297.702	683.722	103.593	424.565	121.362	385.767	361.708
Concentration	248.611	1.766	4.639	1.789	1.58	13.206	226.158		128.915		716.289	0	760.712	
Circular Standard Deviation	3.637	52.525	28.344	50.513	56.303	14.158	2.402		2.607		0.677	106.367	1.309	
Rayleigh Test (Z)	30.875	111.768	278.717	5.516	11.422	12.23	3.993	1	2.994	1	2	0.064	3.998	1
Rayleigh Test (*p*)	<1E-12	<1E-12	<1E-12	0.002	3.53E-06	1.34E-06	0.007	0.512	0.034	0.512	0.137	0.952	0.007	0.512
Rao's Spacing Test (U)	328.913	263.287	312.853	280.608	308.24	282.452	264.139						266.735	
Rao's Spacing Test (*p*)	<0.01	<0.01	<0.01	<0.01	<0.01	<0.01	<0.01						<0.01	
Watson's U^2 Test (von Mises, U^2)	0.366	3.557	15.976	0.465	1.01	0.257								
Watson's U^2 Test (*p*)	<0.005	<0.005	<0.005	<0.005	<0.005	<0.005								
Gage site	Lower lateral													
Behavior	Bite	Chew	Chew	Bite	Bite	Pull	Bite	Bite	Bite	Pull	Pull	Pull	Bite	Bite
Bite point	Right premolar	Left molar	Right molar	Left premolar	Incisors	Incisors	Right Incisors	Left premolar/molar	Right premolar/molar	Left premolar	Right premolar/molar	Right premolar	Right molar	Right canine
n	31	259	356	12	30.0	13	4	1	3	1	2	2	4	1
Mean Vector (μ)	−6.113	68.799	6.834	12.919	−6.5	−20.92	1.127	−10.886	−10.999	−21.39	−7.367	76.198	−8.472	−3.519
Length of Mean Vector (r)	0.871	0.742	0.852	0.641	0.7	0.68	0.996	1	0.998	1	0.999	0.074	0.998	1
Weighted Mean Vector (WMV)	−6.829	57.537	0.169	−4.202	−10.1	−18.169	−2.772	−10.886	−10.64	−21.39	−6.145	−23.085	−9.04	−3.519
Length of WMV (in variable units)	696.899	91.096	349.366	376.42	307.4	125.33	539.493	893.78	1270.491	98.09	458.879	70.14	390.358	301.653
Length of WMV (r, scaled 0–1)	0.429	0.177	0.488	0.403	0.4	0.453	0.428	1	0.868	1	0.611	0.316	0.626	1
ε_1 magnitude mean	710.291	123.909	360.233	466.858	362.9	177.609	542.257	893.78	1272.643	98.09	459.032	152.456	390.988	301.653
ε_1 magnitude standard deviation	404.824	73.334	179.433	276.252	229.3	64.475	481.093		173.49		413.336	98.165	183.085	
ε_1 magnitude maximum	1625	515.514	715.401	933.136	761.8	276.864	1260.38	893.78	1464.08	98.09	751.305	221.869	623.086	301.653
Concentration	4.191	2.296	3.696	1.592	2.17	1.809	50.364		82.979		89.318	0	92.268	
Circular Standard Deviation	30.069	44.289	32.407	54	45.963	50.289	5.097		3.251		1.918	130.675	3.763	
Rayleigh Test (Z)	23.537	142.496	258.532	4.936	15.763	6.017	3.968	1	2.99	1	1.998	0.011	3.983	1
Rayleigh Test (*p*)	2.14E-10	<1E-12	<1E-12	0.005	4.46E-08	0.001	0.007	0.512	0.034	0.512	0.138	0.992	0.007	0.512
Rao's Spacing Test (U)	317.286	241.302	304.511	256.058	305.052	269.447	257.855						259.57	
Rao's Spacing Test (*p*)	<0.01	<0.01	<0.01	<0.01	<0.01	<0.01	<0.01						<0.01	
Watson's U^2 Test (von Mises, U^2)	1.689	1.382	11.533	0.301	1.041	0.472								
Watson's U^2 Test (*p*)	<0.005	<0.005	<0.005	<0.005	<0.005	<0.005								

(*continued on next page*)

Table 5 (*continued*)

Gage site	Medial													
Behavior	Bite	Chew	Chew	Bite	Bite	Pull	Bite	Bite	Bite	Pull	Pull	Pull	Bite	Bite
Bite point	Right premolar	Left molar	Right molar	Left premolar	Incisors	Incisors	Right Incisors	Left premolar/molar	Right premolar/molar	Left premolar	Right premolar/molar	Right premolar	Right molar	Right canine
n	31	259	356	12	30	13	4	1	3	1	2	2	4	1
Mean Vector (μ)	92.36	60.799	89.123	85.179	76.857	89.321	89.411	78.918	90.189	110.414	92.212	79.886	90.76	94.591
Length of Mean Vector (r)	0.986	0.836	0.891	0.988	0.987	0.873	1	1	1	1	1	0.972	0.999	1
Weighted Mean Vector (WMV)	90.083	64.414	91.583	87.085	78.399	85.833	90.133	78.918	90.164	110.414	92.134	86.922	91.053	94.591
Length of WMV (in variable units)	431.463	81.334	262.126	239.219	157.076	92.055	345.84	386.674	602.552	153.203	315.559	94.17	308.308	425.194
Length of WMV (r, scaled 0–1)	0.441	0.277	0.397	0.525	0.512	0.489	0.46	1	0.691	1	0.592	0.65	0.665	1
ε_1 magnitude mean	433.646	97.417	272.314	241.386	158.428	115.134	345.923	386.674	602.604	153.203	315.559	96.198	308.494	425.194
ε_1 magnitude standard deviation	241.091	51.245	124.332	126.745	97.784	46.95	271.003		234.937		307.223	68.87	128.035	
ε_1 magnitude maximum	977.526	293.281	660.229	455.566	306.732	188.305	751.476	386.674	871.856	153.203	532.799	144.897	463.617	425.194
Concentration	36.254	3.387	4.883	32.768	39.581	3.308	956.472		1207.116		25 709.222	1.783	292.732	
Circular Standard Deviation	9.583	34.274	27.525	8.806	9.166	29.905	1.168		0.852		0.113	13.768	2.111	
Rayleigh Test (Z)	30.145	181.088	282.63	11.72	29.242	9.9	3.998	1	2.999	1	2	1.888	3.995	1
Rayleigh Test (*p*)	1.13E-12	<1E-12	<1E-12	1.64E-06	2.57E-12	9.05E-07	0.007	0.512	0.033	0.512	0.137	0.159	0.007	0.512
Rao's Spacing Test (U)	308.606	283.956	308.802	296.516	314.501	281.725	267						265.221	
Rao's Spacing Test (*p*)	<0.01	<0.01	<0.01	<0.01	<0.01	<0.01	<0.01						<0.01	
Watson's U^2 Test (von Mises, U^2)	0.588	4.158	12.377	0.064	0.127	0.419								
Watson's U^2 Test (*p*)	<0.005	<0.005	<0.005	0.5 > p > 0.25	<0.05	<0.005								

Gage site	Neutral axis													
Behavior	Bite	Chew	Chew	Bite	Bite	Pull	Bite	Bite	Bite	Pull	Pull	Pull	Bite	Bite
Bite point	Right premolar	Left molar	Right molar	Left premolar	Incisors	Incisors	Right Incisors	Left premolar/molar	Right premolar/molar	Left premolar	Right premolar/molar	Right premolar	Right molar	Right canine
n	31	259	356	12	30	13	4	1	3	1	2	2	4	1
Mean Vector (μ)	6.724	8.346	8.981	4.866	5.543	6.992	8.653	6.003	6.351	18.296	6.538	7.611	9.393	12.963
Length of Mean Vector (r)	1	0.876	0.994	0.982	1	0.999	1	1	1	1	1	1	0.999	1
Concentration	1174.167	4.321	83.707	21.307	1744.382	482.604	1325.593		12 270.324		1005.141	324.41	211.371	
Circular Standard Deviation	1.672	29.536	6.281	10.956	1.372	2.307	0.992		0.267		0.572	1.006	2.484	
Rayleigh Test (Z)	30.974	198.56	351.747	11.569	29.983	12.979	3.999	1	3	1	2	1.999	3.992	1
Rayleigh Test (*p*)	<1E-12	<1E-12	<1E-12	1.54E-06	1.39E-12	1.25E-06	0.007	0.512	0.033	0.512	0.137	0.137	0.007	0.512
Rao's Spacing Test (U)	341.901	250.799	333.148	286.536	342.223	323.102	267.234						263.979	
Rao's Spacing Test (*p*)	<0.01	<0.01	<0.01	<0.01	<0.01	<0.01	<0.01						<0.01	
Watson's U^2 Test (von Mises, U^2)	0.061	2.26	10.444	0.375	0.071	0.026								
Watson's U^2 Test (*p*)	0.5 > p > 0.25	<0.005	<0.005	<0.005	0.25 > p > 0.15	>0.5								

Table 6
Descriptive statistics for strain data collected during Experiment 184: Chewing data by food.

Gage site	Upper lateral																
Food	Walnut	Brazil nut	Pecan	Hazelnut	Almond	Popcorn	Mango	Apricot	Coconut	Brazil nut	Pecan	Hazelnut	Almond	Popcorn	Mango	Apricot	Coconut
Side	Left									Right							
n	5	61	10.0	67	26	8	26	10	24	97	13	85	25	10	46	15	25
Mean Vector (μ)	239.852	239.666	255.7	260.072	255.949	305.69	205.289	328.93	253.98	292.727	303.044	299.048	293.009	292.467	299.991	299.578	291.602
Length of Mean Vector (r)	0.997	0.628	0.9	0.837	0.93	0.453	0.533	0.872	0.711	0.938	0.771	0.856	0.955	0.999	0.778	0.898	0.982
Weighted Mean Vector (WMV)	240.721	243.645	258.3	263.39	259.924	297.265	352.642	315.037	264.078	291.62	293.007	292.13	291.447	293.221	291.126	290.709	290.017
Length of WMV (in variable units)	40.901	38.154	45.4	59.538	72.57	105.598	20.581	39.792	44.611	237.889	191.294	235.434	246.218	332.371	240.04	129.765	222.437
Length of WMV (r, scaled 0−1)	0.807	0.149	0.6	0.339	0.575	0.464	0.096	0.45	0.526	0.559	0.598	0.542	0.665	0.647	0.489	0.509	0.645
ε_1 magnitude mean	41.006	77.212	48.0	79.184	75.964	169.464	69.636	46.463	52.131	242.498	203.407	240.011	248.29	332.64	248.265	132.545	222.902
ε_1 magnitude standard deviation	9.118	50.184	24.0	36.262	23.21	45.736	53.611	24.331	20.07	109.366	105.67	123.141	81.71	145.032	132.943	73.45	65.877
ε_1 magnitude maximum	50.667	255.587	82.132	175.722	126.185	227.764	215.159	88.427	84.822	425.538	319.858	434.225	370.316	513.726	490.795	254.88	345.04
Concentration	80.528	1.629	5.254	3.404	7.458	0.767	1.263	3.046	2.078	8.299	1.991	3.782	11.312	262.671	2.623	4.21	28.055
Circular Standard Deviation	4.487	55.255	2.21E+01	34.165	21.77	72.135	64.231	2.99E+01	47.3	20.552	41.359	3.20E+01	17.44	3.006	40.55	26.558	10.916
Rayleigh Test (Z)	4.969	24.067	8.623	46.952	22.505	1.64	7.399	7.609	12.14	85.288	7.721	62.272	22.788	9.973	27.876	12.1	24.109
Rayleigh Test (*p*)	0.001	3.53E-11	<1E-12	<1E-12	7.26E-10	0.198	3.87E-04	3.82E-05	1.02E-06	<1E-12	1.10E-04	<1E-12	6.51E-10	<1E-12	2.71E-12	8.69E-07	2.39E-10
Rao's Spacing Test (U)	275.913	266.302	271.641	294.275	287.805	217.079	231.929	267.205	277.477	319.608	266.623	307.098	320.389	313.104	306.517	274.363	323.413
Rao's Spacing Test (*p*)	<0.01	<0.01	<0.01	<0.01	<0.01	<0.01	<0.01	<0.01	<0.01	<0.01	<0.01	<0.01	<0.01	<0.01	<0.01	<0.01	<0.01
Watson's U^2 Test (von Mises, U^2)		0.981	0.371	1.356	0.466		0.072	0.215	0.676	4.319	0.443	3.669	1.377	0.182	1.808	0.501	1.139
Watson's U^2 Test (*p*)		<0.005	<0.005	<0.005	<0.005		0.15 > p > 0.1	<0.005	<0.005	<0.005	<0.005	<0.005	<0.005	<0.01	<0.005	<0.005	<0.005

Gage site	Lower lateral																
Food	Walnut	Brazil nut	Pecan	Hazelnut	Almond	Popcorn	Mango	Apricot	Coconut	Brazil nut	Pecan	Hazelnut	Almond	Popcorn	Mango	Apricot	Coconut
Side	Left									Right							
n	5	61	10	67	26	8	26	10	24	97.0	13	85	25	10	46	15	25
Mean ε_1 orientation (μ)	74.59	79.22	79.244	69.676	75.408	−4.457	57.031	80.521	69.987	6.4	9.623	8.222	−1.007	−5.932	12.646	13.901	4.722
Length of Mean Vector (r)	0.997	0.636	0.994	0.93	0.919	0.256	0.548	0.505	0.708	0.8	0.825	0.865	0.954	0.995	0.866	0.72	0.937
Weighted Mean Vector (WMV)	73.6	63.929	77.976	68.831	75.108	350.035	6.535	22.3	62.023	359.8	0.325	1.122	357.221	352.805	3.227	4.003	3.156
Length of WMV (in variable units)	127.287	52.615	126.318	141.937	146.221	138.585	78.022	35.881	53.189	359.6	318.089	372.214	414.511	378.237	319.215	169.204	307.101
Length of WMV (r, scaled 0−1)	0.794	0.113	0.668	0.603	0.65	0.269	0.211	0.29	0.486	0.5	0.551	0.56	0.689	0.544	0.488	0.496	0.598
ε_1 magnitude mean	127.522	93.268	126.862	150.554	155.215	289.206	103.759	62.11	68.289	375.8	328.944	380.559	419.256	379.556	325.057	183.298	309.405
ε_1 magnitude standard deviation	34.448	70.202	51.011	39.337	40.935	127.771	95.305	41.102	26.334	188.441	174.508	193.063	135.901	180.403	168.701	94.083	112.076
ε_1 magnitude maximum	160.359	466.841	189.178	235.19	225.097	515.514	369.083	123.858	109.352	715.401	577.661	664.113	601.284	695.371	654.285	341.055	513.351
Concentration	83.706	1.664	63.115	7.463	6.486	0.058	1.314	0.993	2.06	3.116	2.508	4.01	11.213	79.821	4.045	1.73	8.184
Circular Standard Deviation	4.401	5.45E+01	6.145	21.762	23.489	94.573	62.823	6.70E+01	4.76E+01	36.19	35.509	30.863	17.521	5.461	3.07E+01	46.439	2.07E+01
Rayleigh Test (Z)	4.971	24.653	9.886	58	21.978	0.525	7.814	2.547	12.046	65.089	8.854	63.593	22.768	9.91	34.518	7.777	21.939
Rayleigh Test (*p*)	0.001	1.96E-11	<1E-12	<1E-12	1.07E-09	0.607	2.38E-04	0.075	1.14E-06	<1E-12	1.34E-05	<1E-12	6.60E-10	<1E-12	<1E-12	1.38E-04	1.22E-09
Rao's Spacing Test (U)	276.069	218.129	299.868	297.951	285.75	256.967	256.051	255.444	211.745	305.755	290.945	318.906	314.708	303.877	297.836	245.351	310.748
Rao's Spacing Test (*p*)	<0.01	<0.01	<0.01	<0.01	<0.01	<0.01	<0.01	<0.01	<0.01	<0.01	<0.01	<0.01	<0.01	<0.01	<0.01	<0.01	<0.01

(*continued on next page*)

Table 6 (*continued*)

Gage site	Lower lateral																
Food	Walnut	Brazil nut	Pecan	Hazelnut	Almond	Popcorn	Mango	Apricot	Coconut	Brazil nut	Pecan	Hazelnut	Almond	Popcorn	Mango	Apricot	Coconut
Side	Left									Right							
Watson's U^2 Test (von Mises, U^2)		0.193	0.211	1.604	0.655		0.309	0.208	0.066	3.39	0.512	3.384	1.035	0.072	1.142	0.466	0.983
Watson's U^2 Test (p)		<0.005	<0.005	<0.005	<0.005		<0.005	<0.005	0.25 > p > 0.15	<0.005	<0.005	<0.005	<0.005	0.25 > p > 0.15	<0.005	<0.005	<0.005
Gage site	Lower lateral									Lower lateral							
Food	Walnut	Brazil nut	Pecan	Hazelnut	Almond	Popcorn	Mango	Apricot	Coconut	Brazil nut	Pecan	Hazelnut	Almond	Popcorn	Mango	Apricot	Coconut
Side	Left									Right							
n	5	61	10	67	26	8	26	10	24	97.0	13	85	25	10	46	15	25
Mean Vector (μ)	74.59	79.22	79.244	69.676	75.408	−4.457	57.031	80.521	69.987	6.4	9.623	8.222	−1.007	−5.932	12.646	13.901	4.722
Length of Mean Vector (r)	0.997	0.636	0.994	0.93	0.919	0.256	0.548	0.505	0.708	0.8	0.825	0.865	0.954	0.995	0.866	0.72	0.937
Weighted Mean Vector (WMV)	73.6	63.929	77.976	68.831	75.108	−10.04	6.535	22.3	62.023	−0.2	0.325	1.122	−2.8	−7.2	3.227	4.003	3.156
Concentration	83.706	1.664	63.115	7.463	6.486	0.058	1.314	0.993	2.06	3.116	2.508	4.01	11.213	79.821	4.045	1.73	8.184
Circular Standard Deviation	4.401	5.45E+01	6.145	21.762	23.489	94.573	62.823	6.70E+01	4.76E+01	36.19	35.509	30.863	17.521	5.461	3.07E+01	46.439	2.07E+01
Rayleigh Test (Z)	4.971	24.653	9.886	58	21.978	0.525	7.814	2.547	12.046	65.089	8.854	63.593	22.768	9.91	34.518	7.777	21.939
Rayleigh Test (p)	0.001	1.96E-11	<1E-12	<1E-12	1.07E-09	0.607	2.38E-04	0.075	1.14E-06	<1E-12	1.34E-05	<1E-12	6.60E-10	<1E-12	<1E-12	1.38E-04	1.22E-09
Rao's Spacing Test (U)	276.069	218.129	299.868	297.951	285.75	256.967	256.051	255.444	211.745	305.755	290.945	318.906	314.708	303.877	297.836	245.351	310.748
Rao's Spacing Test (p)	<0.01	<0.01	<0.01	<0.01	<0.01	<0.01	<0.01	<0.01	<0.01	<0.01	<0.01	<0.01	<0.01	<0.01	<0.01	<0.01	<0.01
Watson's U^2 Test (von Mises, U^2)		0.193	0.211	1.604	0.655		0.309	0.208	0.066	3.39	0.512	3.384	1.035	0.072	1.142	0.466	0.983
Watson's U^2 Test (p)		<0.005	<0.005	<0.005	<0.005		<0.005	<0.005	0.25 > p > 0.15	<0.005	<0.005	<0.005	<0.005	0.25 > p > 0.15	<0.005	<0.005	<0.005
Gage site	Medial									Medial							
Food	Walnut	Brazil nut	Pecan	Hazelnut	Almond	Popcorn	Mango	Apricot	Coconut	Brazil nut	Pecan	Hazelnut	Almond	Popcorn	Mango	Apricot	Coconut
Side	Left									Right							
n	5	61.0	10	67	26	8	26	10	24	97	13	85	25	10	46	15	25
Mean Vector (μ)	49.746	60.2	59.547	66.861	59.473	72.952	42.04	6.799	72.675	91.426	83.641	91.505	87.009	95.725	82.775	83.437	88.796
Length of Mean Vector (r)	0.999	0.8	0.892	0.931	0.914	0.997	0.697	0.61	0.823	0.888	0.757	0.893	0.941	0.99	0.855	0.783	0.937
Weighted Mean Vector (WMV)	50.381	62.8	54.103	69.464	58.623	73.171	56.288	−0.161	74.091	92.831	90.097	92.745	88.666	94.379	90.82	86.76	90.253
Length of WMV (in variable units)	61.413	81.7	56.642	85.519	82.514	39.329	68.529	61.642	49.906	264.55	216.131	263.813	265.094	440.871	297.324	146.783	242.682
Length of WMV (r, scaled 0–1)	0.767	0.3	0.521	0.374	0.519	0.748	0.263	0.477	0.562	0.522	0.586	0.544	0.656	0.668	0.468	0.481	0.645
ε_1 magnitude mean	61.453	103.4	67.648	92.764	93.417	220.03	94.563	96.78	64.422	280.098	245.993	271.926	271.116	442.438	303.38	166.02	248.232
ε_1 magnitude standard deviation	18.141	46.562	31.956	43.226	35.603	48.443	57.122	17.875	16.212	112.707	101.157	129.932	84.744	173.797	161.813	70.619	64.933
ε_1 magnitude maximum	80.105	260.685	108.716	228.871	159.004	293.281	260.721	129.19	88.751	506.356	368.854	485.268	403.907	660.229	635.566	305.29	376.157
Concentration	267.877	2.835	3.543	7.549	6.075	96.999	1.985	1.421	3.173	4.751	1.896	4.964	8.703	36.813	3.752	2.162	8.237
Circular Standard Deviation	2.457	38.514	27.444	21.627	24.351	4.733	4.87E+01	56.974	35.766	27.958	42.712	27.268	20.037	8.063	3.21E+01	4.01E+01	20.635
Rayleigh Test (Z)	4.991	38.823	7.95	58.103	21.703	7.946	12.614	3.72	16.255	76.448	7.458	67.772	22.122	9.804	33.599	9.198	21.959
Rayleigh Test (p)	0.001	<1E-12	8.07E-06	<1E-12	1.30E-09	<1E-12	6.84E-07	0.02	5.36E-08	<1E-12	1.67E-04	<1E-12	1.06E-09	<1E-12	<1E-12	1.49E-05	1.20E-09
Rao's Spacing Test (U)	281.256	297.86	273.85	305.287	311.023	298.078	275.503	266.517	285.099	298.68	290.03	314.225	318.219	290.812	304.422	262.44	316.71
Rao's Spacing Test (p)	<0.01	<0.01	<0.01	<0.01	<0.01	<0.01	<0.01	<0.01	<0.01	<0.01	<0.01	<0.01	<0.01	<0.01	<0.01	<0.01	<0.01
Watson's U^2 Test (von Mises, U^2)		0.973	0.409	1.036	0.938		0.332	0.248	0.496	3.318	0.497	3.414	1.199	0.157	1.631	0.451	1.142
Watson's U^2 Test (p)		<0.005	<0.005	<0.005	<0.005		<0.005	<0.005	<0.005	<0.005	<0.005	<0.005	<0.005	<0.025	<0.005	<0.005	<0.005

Gage site: Neutral axis

Food	Walnut	Brazil nut	Pecan	Hazelnut	Almond	Popcorn	Mango	Apricot	Coconut	Brazil nut	Pecan	Hazelnut	Almond	Popcorn	Mango	Apricot	Coconut
Side					Left								Right				
n	5	61	10	67	26	8	26	10	24	97	13	85	25	10	46	15	25
Mean Vector (μ)	11.1	8.303	−17.401	11.145	5.609	12.292	8.07	7.174	12.283	9.454	7.718	8.602	8.837	13.435	9.436	8.138	9.821
Length of Mean Vector (r)	0.7	0.922	0.823	0.727	0.845	0.997	0.985	0.992	0.992	0.986	0.999	0.999	1	1	0.999	0.999	0.999
Concentration	1.67	6.712	2.286	2.189	3.556	103.573	32.697	45.864	65.593	36.634	316.403	403.009	1557.108	814.686	496.182	288.451	655.575
Circular Standard Deviation	50.426	23.053	35.811	45.707	33.207	4.58	10.099	7.216	7.102	9.532	2.85	2.856	1.452	1.706	2.573	3.037	2.239
Rayleigh Test (Z)	2.305	51.883	6.766	35.456	18.582	7.949	25.205	9.843	23.634	94.352	12.968	84.789	24.984	9.991	45.907	14.958	24.962
Rayleigh Test (p)	0.096	<1E-12	2.71E-04	<1E-12	1.09E-08	<1E-12	9.29E-11	<1E-12	3.81E-10	<1E-12	1.26E-06	<1E-12	1.21E-10	<1E-12	<1E-12	3.98E-07	1.24E-10
Rao's Spacing Test (U)	142.862	275.878	209.099	205.824	226.211	299.357	321.338	299.547	310.298	322.989	322.276	340.973	337.484	318.692	340.348	325.317	331.238
Rao's Spacing Test (p)	0.50 > p > 0.10	<0.01	<0.01	<0.01	<0.01	<0.01	<0.01	<0.01	<0.01	<0.01	<0.01	<0.01	<0.01	<0.01	<0.01	<0.01	<0.01
Watson's U^2 Test (von Mises, U^2)		1.056	0.095	0.074	0.059		0.539	0.247	0.092	3.96	0.208	1.855	0.263	0.038	0.421	0.226	0.258
Watson's U^2 Test (*p*)			<0.005	<0.005	<0.005	>0.5	<0.005	<0.005	<0.005	<0.005	<0.005	0.1 > p > 0.05	0.25 > p > 0.15	0.5 >p > 0.25		<0.005	0.15 >p > 0.1

animals in this study, especially during ingestion cycles when the shells were broken by the animals. Moreover, we do not know whether we have sampled the high-end range of FMPs ingested and chewed by tufted capuchins in the wild (Wright, 2005a, b; Wright et al., 2009; Chalk et al., 2016). However, these limitations do not impact the analyses performed in this study as FMP data were not included in the statistical analyses.

What do the results presented here mean for the three hypotheses presented in Introduction?

7.1. Variation in strain regimes due to variation in feeding behavior

The first hypothesis, that variation in oral food processing behaviors elicits significant variation in strain regimes in the mandibular corpus, is corroborated. Variation in oral food processing behavior—represented here by "cycle type," including biting and/or pulling at incisors, premolars, and molars, as well as chewing—had significant effects on ε_1 strain magnitudes at all gage sites, in all experiments, except the medial gage in Experiment 183. Moreover, in all experiments at all gage sites, the largest strain magnitudes were recorded during biting, not chewing. When the highest peak strain magnitudes are considered (whiskers in Fig. 11), the behaviors with the highest strains in Experiments 184 and 185 were incisor biting and ipsilateral and contralateral premolar biting, whereas in Experiment 183 the highest peak strain magnitudes at all gage sites were recorded during contralateral molar biting. When highest mean strain magnitudes are considered, ipsilateral molar and premolar biting are associated with the highest magnitudes at all gage sites.

Cycle type variation significantly affected $|\varepsilon_1/\varepsilon_2|$ ratios at the upper lateral gage site in Experiment 184, at the two lateral gage sites in Experiment 183, and at all three gage sites in Experiment 185. Cycle type variation also significantly affected ε_1 orientation at seven out of nine gage sites (not at the lateral gage sites in Experiment 185) and the orientation of the neutral axis of bending in Experiment 183, but not 184 or 185. The neutral axis of bending is the axis about which the mandible is bent, so low variation in its orientation suggests that variation in strain orientations and $|\varepsilon_1/\varepsilon_2|$ ratios (see below) reflects variation in other deformation regimes, such as twisting and shear.

In addition, in Experiments 183 and 184, the interaction between food and cycle type had significant effects on ε_1 magnitude at all gage sites except the medial gage in Experiment 183, and on $|\varepsilon_1/\varepsilon_2|$ ratios at all gage sites. This interaction effect means that the way that food type affects strain magnitudes and principal strain ratios depends on the cycle type, and the way that cycle type affects strain regimes depends on the food being eaten.

Macaque mandibular corpus strain orientations have been shown to vary little across the oral food processing and transducer biting behaviors sampled: chewing, ingestive incisor biting, and isometric transducer biting on incisors and molars (Fig. 1; Hylander, 1979a, b). However, the variation across behaviors in the macaque studies is narrower than that documented here. This may be because a narrower range of behaviors was sampled in the macaque studies and/or because their hands were restrained, whereas the capuchins studied here used their hands to feed. It remains to be determined whether macaques would employ as wide a range of feeding behaviors as capuchins under the same experimental conditions, and whether these would result in as wide a range of mandibular loading and strain regimes.

The second hypothesis we evaluated was whether the mastication of foods with different material properties is associated with significant variation in strain regimes in the mandibular corpus. This hypothesis received mixed support. There were only significant effects for food type on strain regimes at the upper lateral and

Table 7
Experiment 185 data by behavior.

Gage site	Upper lateral				
Behavior	Chew		Bite		
Bite point	Left molar	Right molar	Incisors	Left premolar	Right premolar
n	102	82	12	9	4
Mean Vector (μ)	65.7	65.2	66.0	66.9	68.4
Length of Mean Vector (r)	0.983	0.712	1	0.997	1
Weighted Mean Vector (WMV)	65.419	68.153	65.839	66.775	68.049
Length of WMV (in variable units)	333.078	159.309	596.477	761.094	745.735
Length of WMV (r, scaled 0–1)	0.533	0.345	0.505	0.675	0.725
ε_1 magnitude mean	334.624	179.76	596.755	763.111	745.824
ε_1 magnitude standard deviation	129.262	101.902	336.035	291.411	292.869
ε_1 magnitude maximum	625.249	461.67	1180.22	1127.38	1028.27
Concentration	30.288	2.082	899.65	132.612	979.743
Circular Standard Deviation	10.5	47.2	1.7	4.2	1.2
Rayleigh Test (Z)	98.632	41.552	11.99	8.953	3.998
Rayleigh Test (*p*)	<1E-12	<1E-12	1.75E-06	<1E-12	0.007
Rao's Spacing Test (U)	335.044	294.533	325.473	308.454	267.21
Rao's Spacing Test (*p*)	<0.01	<0.01	<0.01	<0.01	<0.01
Watson's U^2 Test (von Mises, U^2)	4.041	2.083	0.106		
Watson's U^2 Test (p)	<0.005	<0.005	0.1 > p > 0.05		
Gage site	Lower lateral				
Behavior	Chew		Bite		
Bite point	Left molar	Right molar	Incisors	Left premolar	Right premolar
n	102	82	12	9	4
Mean Vector (μ)	76.4	78.9	73.2	75.0	73.1
Length of Mean Vector (r)	0.978	0.759	0.999	0.996	1
Weighted Mean Vector (WMV)	76.874	81.251	73.222	74.808	73.337
Length of WMV (in variable units)	123.57	74.89	130.972	169.396	163.273
Length of WMV (r, scaled 0–1)	0.601	0.39	0.551	0.733	0.677
ε_1 magnitude mean	124.648	81.779	131.13	170.037	163.345
ε_1 magnitude standard deviation	48.222	50.257	58.969	61.133	72.605
ε_1 magnitude maximum	205.545	191.852	237.499	231.082	241.289
Concentration	22.617	2.44	273.602	93.442	413.195
Circular Standard Deviation	12.2	42.5	3.0	4.9	1.8
Rayleigh Test (Z)	97.489	47.251	11.966	8.933	3.996
Rayleigh Test (*p*)	<1E-12	<1E-12	1.74E-06	<1E-12	0.007
Rao's Spacing Test (U)	323.625	306.02	319.264	305.923	265.873
Rao's Spacing Test (*p*)	<0.01	<0.01	<0.01	<0.01	<0.01
Watson's U^2 Test (von Mises, U^2)	4.245	2.743	0.033		
Watson's U^2 Test (*p*)	<0.005	<0.005	>0.5		
Gage site	Medial				
Behavior	Chew		Bite		
Bite point	Left molar	Right molar	Incisors	Left premolar	Right premolar
n	102	82	12	9	4
Mean Vector (μ)	36.1	75.7	34.4	42.7	48.4
Length of Mean Vector (r)	0.83	0.85	0.925	0.973	0.999
Weighted Mean Vector (WMV)	25.624	71.4	30.734	47.402	49.126
Length of WMV (in variable units)	161.745	101.785	223.564	376.859	498.977
Length of WMV (r, scaled 0–1)	0.463	0.397	0.615	0.639	0.688
ε_1 magnitude mean	175.363	117.988	240.929	383.901	499.393
ε_1 magnitude standard deviation	88.246	57.975	79.384	202.582	206.396
ε_1 magnitude maximum	349.573	256.158	363.521	589.746	725.635
Concentration	3.283	3.644	5.287	12.816	140.603
Circular Standard Deviation	35.0	32.7	22.7	13.5	3.0
Rayleigh Test (Z)	70.269	59.214	10.259	8.513	3.989
Rayleigh Test (*p*)	<1E-12	<1E-12	<1E-12	<1E-12	0.007
Rao's Spacing Test (U)	262.566	260.896	246.975	271.976	261.853
Rao's Spacing Test (*p*)	<0.01	<0.01	<0.01	<0.01	<0.01
Watson's U^2 Test (von Mises, U^2)	1.803	0.303	0.07		
Watson's U^2 Test (*p*)	<0.005	<0.005	0.25 > p > 0.15		
Gage site	Neutral axis				
Behavior	Chew		Bite		
Bite point	Left molar	Right molar	Incisors	Left premolar	Right premolar
n	102	82	12	9	4
Mean Vector (μ)	346.5	336.6	348.6	345.0	341.0
Length of Mean Vector (r)	0.95	0.725	0.984	0.995	0.998
Concentration	10.267	2.174	23.959	64.075	112.888
Circular Standard Deviation	18.4	45.9	10.3	6.0	3.4
Rayleigh Test (Z)	92.053	43.151	11.617	8.903	3.986

Table 7 (*continued*)

Gage site	Neutral axis				
Behavior	Chew		Bite		
Bite point	Left molar	Right molar	Incisors	Left premolar	Right premolar
Rayleigh Test (p)	<1E-12	<1E-12	1.57E-06	<1E-12	0.007
Rao's Spacing Test (U)	301.827	250.068	290.136	301.191	260.961
Rao's Spacing Test (p)	<0.01	<0.01	<0.01	<0.01	<0.01
Watson's U^2 Test (von Mises, U^2)	1.46	0.604	0.307		
Watson's U^2 Test (p)	<0.005	<0.005	<0.005		

Table 8a
Results of three-way ANOVA of effects of cycle number, cycle type[a], and food type on ε_1 strain magnitude and $|\varepsilon_1/\varepsilon_2|$ ratio.

Exp 183												
Gauge location	Upper lateral gauge				Lower lateral gauge				Medial gauge			
Variable	ε_1 magnitude		$\varepsilon_1/\varepsilon_2$		ε_1 magnitude		$\varepsilon_1/\varepsilon_2$		ε_1 magnitude		$\varepsilon_1/\varepsilon_2$	
Statistic	F	Sig.	F	Sig.	F	Sig.	F	Sig.	F	Sig.	F	Sig.
Intercept	46.1	<.001	56.3	<.001	63.6	<.001	28.5	.001	40.3	<.001	0.1	.790
Cycle number (covariate)	16.2	<.001	0.1	ns	23.2	<.001	14.9	<.001	38.9	<.001	31.8	<.001
Cycle type (random)	6.7	.009	50.1	<.001	5.2	.011	8.4	.001	2.0	ns	0.5	ns
Food (random)	2.0	ns	1.2	ns	2.3	ns	4.3	.039	7.3	.006	13.6	.001
Cycle type × food interaction	8.3	<.001	3.2	.005	4.2	<.001	3.5	.002	2.1	ns	3.6	.002
Exp 184												
Gauge location	Upper lateral gauge				Lower lateral gauge				Medial gauge			
Variable	ε_1 magnitude		$\varepsilon_1/\varepsilon_2$		ε_1 magnitude		$\varepsilon_1/\varepsilon_2$		ε_1 magnitude		$\varepsilon_1/\varepsilon_2$	
Statistic	F	Sig.	F	Sig.	F	Sig.	F	Sig.	F	Sig.	F	Sig.
Intercept	126.0	<.001	52.7	<.001	139.3	<.001	0.2	.641	128.5	<.001	4.6	.041
Cycle number (covariate)	21.5	<.001	5.6	.018	16.3	<.001	25.3	<.001	21.2	<.001	18.8	<.001
Cycle type (random)	17.3	<.001	2.1	.030	16.5	<.001	1.6	ns	15.5	<.001	2.5	.011
Food (random)	3.7	.002	3.4	.003	3.0	.008	1.0	ns	3.8	.002	1.3	ns
Cycle type × food interaction	2.3	.001	2.3	.001	2.9	<.001	4.5	<.001	2.8	<.001	3.2	<.001

[a] Cycle type includes type (chew, bite, pull) and point (left molar, left premolar, left canine, incisors, right molar, right premolar, right canine).

medial gage sites in Experiment 184, and these effects were characterized by low F-values (Table 8b). During chewing cycles, the largest effects on ε_1 magnitudes were always cycle number and/or chewing side. Similarly, out of all the six gage sites in Experiments 183 and 184 food type only significantly affected $|\varepsilon_1/\varepsilon_2|$ ratios at the medial gage site in Experiment 183 (Table 8b). Again, chew side or cycle number had larger effects on $|\varepsilon_1/\varepsilon_2|$ ratios than did food type. Chew side had a significant effect on ε_1 orientations at all gage sites during all experiments, except the lateral gage sites in Experiment 185. Controlling for chew side, food type had a significant effect on ε_1 orientations at two out of six working side gage sites (i.e., the working side medial and lower lateral gage sites in Experiment 183), at four out of six balancing side gage sites (i.e., the balancing side medial and upper lateral gage sites in both Experiments 183 and

Table 8b
Results of two-way ANOVA of effects of cycle number, chew side, and food type on ε_1 strain magnitude and $\varepsilon_1/\varepsilon_2$ ratio during chewing cycles.

Exp 183												
Gauge location	Upper lateral gauge				Lower lateral gauge				Medial gauge			
Variable	ε_1 magnitude		$\varepsilon_1/\varepsilon_2$		ε_1 magnitude		$\varepsilon_1/\varepsilon_2$		ε_1 magnitude		$\varepsilon_1/\varepsilon_2$	
Statistic	F	Sig.	F	Sig.	F	Sig.	F	Sig.	F	Sig.	F	Sig.
Intercept	88.8	.001	37.4	<.001	124.1	<.001	21.1	.014	87.0	.001	0.4	0.572
Cycle number (covariate)	36.5	<.001	0.1	ns	41.7	<.001	14.7	<.001	42.1	<.001	31.6	<.001
Side (fixed)	26.5	.013	124.2	.001	14.9	.028	14.0	.031	1.7	ns	0.0	ns
Food type (random)	1.8	ns	0.6	ns	2.4	ns	4.0	ns	7.1	ns	10.3	0.042
Chew side × food type	9.4	<.001	3.9	.009	6.4	<.001	6.9	<.001	3.3	.020	5.7	0.001
Exp 184												
Gauge location	Upper lateral gauge				Lower lateral gauge				Medial gauge			
Variable	ε_1 magnitude		$\varepsilon_1/\varepsilon_2$		ε_1 magnitude		$\varepsilon_1/\varepsilon_2$		ε_1 magnitude		$\varepsilon_1/\varepsilon_2$	
Statistic	F	Sig.	F	Sig.	F	Sig.	F	Sig.	F	Sig.	F	Sig.
Intercept	234.8	<.001	9.7	.007	218.5	<.001	9.7	.007	236.6	<.001	35.6	<.001
Cycle number (covariate)	30.3	<.001	21.6	<.001	27.0	<.001	21.6	<.001	31.1	<.001	18.2	<.001
Side (fixed)	279.1	<.001	0.2	ns	102.9	<.001	0.2	ns	193.2	<.001	7.1	.026
Food type (random)	7.1	.003	0.7	ns	3.1	ns	0.7	ns	5.3	.014	1.2	ns
Chew side × food type	0.8	ns	11.6	<.001	2.2	.031	11.6	<.001	1.6	ns	6.3	<.001

Table 9
Results of one-way ANOVA of effects of cycle type, with cycle number as a covariate, on ε_1 strain magnitude and $|\varepsilon_1/\varepsilon_2|$ ratio in Experiment 185.

Gauge location	Upper lateral gauge				Lower lateral gauge				Medial gauge			
Variable	ε_1 magnitude		$\varepsilon_1/\varepsilon_2$		ε_1 magnitude		$\varepsilon_1/\varepsilon_2$		ε_1 magnitude		$\varepsilon_1/\varepsilon_2$	
Statistic	F	Sig.	F	Sig.	F	Sig.	F	Sig.	F	Sig.	F	Sig.
Intercept	47.3	.001	99.1	.000	77.9	.000	0.9	ns	59.3	.001	4.2	ns
Cycle type (random)	38.3	.000	9.0	.000	11.2	.000	12.1	.000	26.1	.000	11.1	.000
Cycle number (covariate)	3.0	ns	9.9	.002	0.0	ns	32.9	.000	2.1	ns	5.5	.020

Table 10
Measures of variation in ε_1 orientations (in degrees).[a]

	All non-chews	All chews	Left chews (balancing side)	Right chews (working side)
Circular standard deviations of ε_1 orientations.				
Experiment 183				
Upper lateral gauge	*35*	**43**	30	31
Lower lateral gauge	**92**	*71*	43	27
Medial gauge	20	**23**	**23**	*21*
Neutral axis	*26*	20	**28**	11
Experiment 184				
Upper lateral gauge	52	**78**	*53*	28
Lower lateral gauge	**52**	*50*	44	32
Medial gauge	19	**35**	**35**	*29*
Neutral axis	6	*20*	**31**	6
Range of mean ε_1 orientations.				
Experiment 183				
Upper lateral gauge	*81*	**132**	26	4
Lower lateral gauge	*81*	**140**	18	15
Medial gauge	**46**	*41*	28	36
Neutral axis	**30**	*24*	15	16
Experiment 184				
Upper lateral gauge	*106*	**124**	**124**	11
Lower lateral gauge	**98**	*86*	85	20
Medial gauge	37	**89**	*66*	13
Neutral axis	13	**31**	*30*	6
Range of weighted mean ε_1 orientations.				
Experiment 183				
Upper lateral gauge	*92*	**136**	26	92
Lower lateral gauge	*112*	**142**	84	72
Medial gauge	*37*	**46**	34	35
Experiment 184				
Upper lateral gauge	*15*	**112**	**112**	3
Lower lateral gauge	*20*	**88**	**88**	11
Medial gauge	32	**95**	*74*	8

[a] Highest value in each row is in bold, second highest value in each row is in italics.

184), and on neutral axis orientation on both working and balancing sides in Experiment 183, but on neither side in Experiment 184. Food/FMP effects on strain regimes during chewing were more common in Experiment 183 than Experiment 184, more common at balancing side than working side gage sites, and more common for ε_1 orientations than ε_1 magnitudes or $|\varepsilon_1/\varepsilon_2|$ ratios. Thus, although chewing different foods was associated with variation in strain regimes, as predicted by Hypothesis 2, chew side and chew number had larger effects than did food type. Indeed, in Experiments 183 and 184 food type had the smallest (mostly non-significant) effects on ε_1 magnitudes and $|\varepsilon_1/\varepsilon_2|$ ratios of any of the factors.

The third hypothesis that we evaluated was whether the variation in strain regimes associated with different oral food processing behaviors is greater than that during chewing on different foods with different material properties. The three metrics used to quantify relative variability were the circular standard deviation (S), the range of mean ε_1 orientations, and the range of weighted mean ε_1 orientations. The relative variability of strain regimes across different behaviors versus chewing on different foods differs depending on the metric, the individual, and the gage site, nevertheless several patterns can be observed. First, in the majority of the 22 comparisons in Table 10, the widest range or greatest standard deviation in ε_1 orientations is across all chews combined, i.e., working and balancing sides combined. This suggests that there is often more variation in strain regimes with chewing side than between different feeding behaviors. Variation in mastication-related strain regimes with chew side is documented for the mandibular corpus of macaques, galagos, and owl monkeys (Hylander, 1979a, b, c; Hylander et al., 1998) and for the mandibular symphysis of macaques (Hylander, 1984). In macaques, these strain data suggest that the working or biting side mandibular corpus in the molar region is "primarily twisted about its long axis, directly sheared dorsoventrally, and slightly bent in both parasagittal and transverse planes during the power stroke of both mastication and unilateral molar biting" (Hylander, 1988: 56), whereas "the balancing-side mandibular corpus in the molar region is primarily twisted about its long axis, directly sheared dorsoventrally, and powerfully bent in the parasagittal plane during the power stroke of both mastication and unilateral biting" (Hylander, 1988: 56–57). Thus, in macaques, the working side corpus is subjected to

relatively greater twisting and the balancing side corpus to relatively greater bending. What are the implications of such working-balancing side differences in deformation regimes for mandibular design in primates? If individual primates spend approximately equal amounts of time chewing on left and right sides, and mandibular corpus morphology reflects adaptations to resist chewing stresses and strains, then mandibular corpus geometry must be a trade-off between resistance to twisting and resistance to parasagittal bending. Exactly how this trade-off would be manifested is difficult to predict, but it does raise the possibility that working/balancing side variation in strain regimes could mask dietary effects on mandibular corpus morphology.

Second, in the majority of cases in Table 10, variation in chewing related strain regimes is greater on the balancing side than the working side, and in Experiment 184, the highest strain magnitudes at all gage sites were recorded during ipsilateral premolar biting. This might suggest that working side strain regimes have a more consistent and stronger effect on mandibular corpus design than balancing side strain regimes, predicting greater diet-related variation in the degree of resistance to torsional stress than bending stress. Unfortunately, the exact nature of the relationship between torsional stress and mandibular morphology in primates is unclear (Daegling and Hylander, 1991). Moreover, an argument can be marshalled that high bending stresses on the balancing side corpus associated with contralateral chewing and biting might be important in driving mandibular corpus morphology. As summarized in the Introduction, relatively deep mandibular corpora relative to incisor load arms characterize the mandibles of both hard object feeding orangutans and *Lophocebus*, and the highest strains in Experiment 184 were at the upper lateral gage site during contralateral biting. If bending is the predominant loading regime in the balancing side corpus in these animals as in macaques, this might reflect a greater importance of balancing side loading regimes. The significance of this greater variation in balancing side strain regimes is therefore unclear.

Third, if the effects of chew side on variation in strain regimes are ignored, the range of ε_1 orientations across different feeding behaviors exceed those recorded during chewing on either side in 10 of 22 cases, and exceed those recorded on at least one side in 19 of 22 cases. These data do not provide strong support for the hypothesis that variation in strain regimes associated with different behaviors always exceeds variation associated with chewing on different foods, but they do suggest that variation in strain regimes associated with different feeding behaviors can exceed that associated with chewing on different foods. Stronger support for the third hypothesis comes from previously published data on macaques (Hylander, 1979c), in which strain orientations recorded from the lateral aspect of the mandibular corpus show less variation during mastication of different foods ($<2^\circ$) than across different behaviors (Fig. 1; Hylander, 1979c; average difference $= 26^\circ$ in Table 8). Moreover, published data from non-

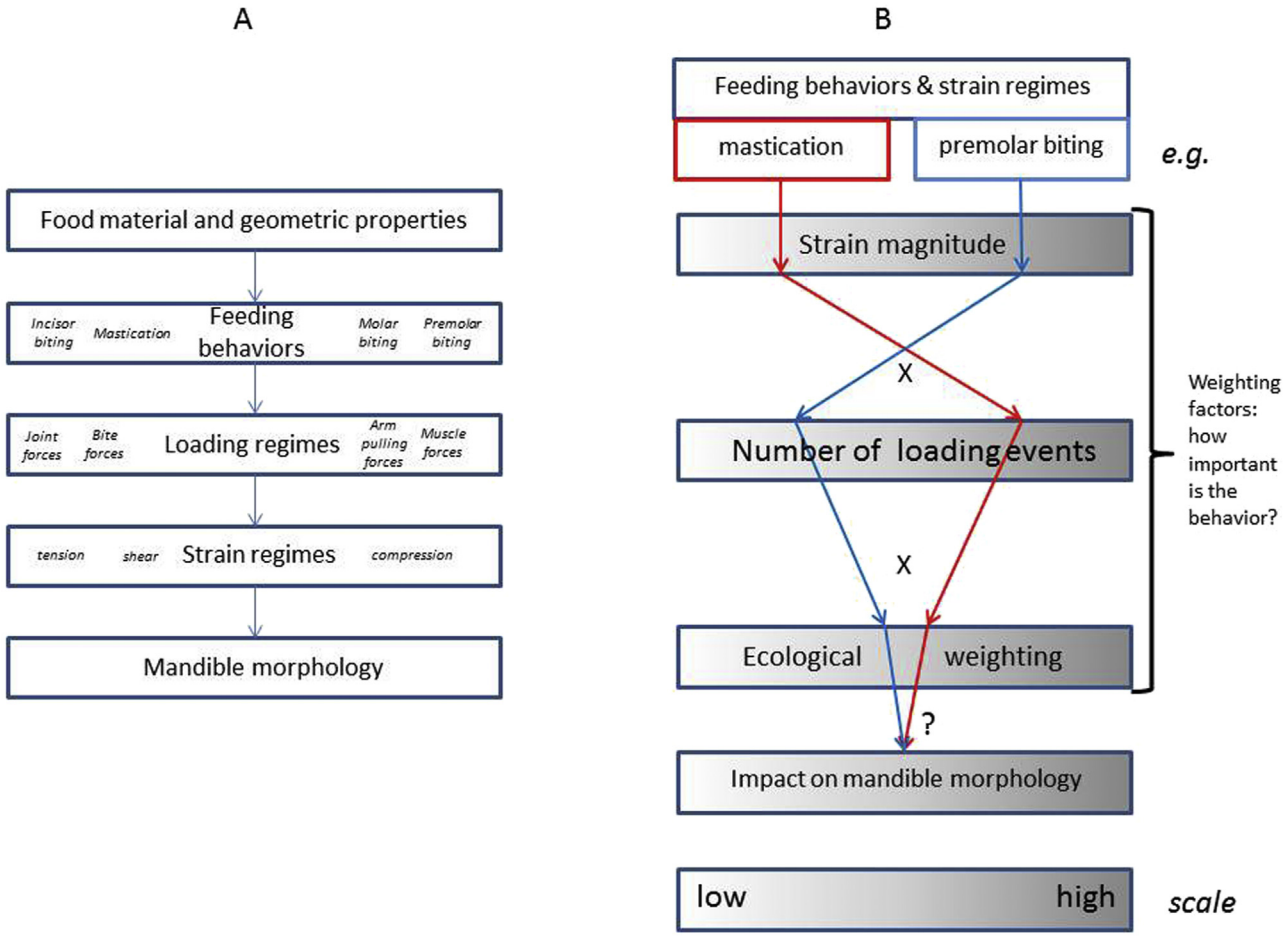

Figure 12. A) Food material and geometric properties can only impact mandible morphology by eliciting variation in feeding behaviors that in turn result in differences in mandibular loading and strain regimes. B) The relative importance of these different behaviors for mandible morphology depends on weighting factors, including biomechanical variables such as strain magnitude and the amount of time or number of times the mandible is subjected to a given strain regime. A range of ecological variables can also weight the importance of the behavior, such as whether the resource is *necessary* for survival (e.g., a fall-back food).

primate mammals suggest that their mandibles also experience low levels of variation in strain regimes during mastication of different foods. Williams et al. (2011) report no significant differences between strain orientations and $|\varepsilon_1/\varepsilon_2|$ ratios recorded during rumination chewing and ingestion chewing in goats (Williams et al., 2011).[2] In rabbits, mean working side ε_2 orientations varied by only 1° across chewing of pellets (33° relative to occlusal plane), hay (34°), and carrot (33°); balancing side ε_2 orientations varied more (pellets, 73°; hay, 76°; carrot 92°), while strain orientations during carrot incision were very different (49°; Weijs and De Jong, 1977). Collectively these data from non-primate mammals suggest that strain regimes in the mammalian mandible often vary little between chews on different foods/FMPs and are more strongly affected by chewing side and, where data are available, chew number.

Finally, it is worth noting that consideration of the standard deviations in Table 10 reveals interesting patterns in variability in strain and neutral axis orientation. In both Experiments 183 and 184, the highest values of ε_1 orientation S were found: at the upper lateral gage site across all chew cycles (working and balancing sides pooled), at the lower lateral gage site across all non-chew cycles, and at the medial gage site and neutral axis across contralateral chews. Confirmation of this pattern might suggest differences in relative importance of different behaviors for the morphology of different parts of the mandible.

8. What do our results reveal about primate mandibular corpus form-function relationships?

In order for interspecific variation in mandibular (in this case corpus) morphology to be consistently related to interspecific variation in the material or geometric properties of primate foods, three criteria must be met (Ross et al., 2012; Ross and Iriarte-Diaz, 2014: Fig. 12). First, variation in food geometric and/or material properties must elicit variation in feeding behavior that results in variation in mandibular corpus loading regimes (patterns of external forces acting on the corpus) that are in turn associated with variation in mandibular corpus stress and strain regimes. For example, if two foods are of similarly high toughness and Young's modulus, but one (perhaps the larger) is consistently ingested via biting on the premolars while the other is consistently ingested via biting on the molars, then the differences in food geometric properties do elicit different feeding behaviors characterized by different mandibular loading regimes (different bite points by definition imply different loading regimes, with or without different jaw-muscle activity patterns). Similarly, if foods with different material properties are chewed in different ways, this might elicit variation in mandibular corpus loading regimes. If these different loading regimes result in different strain regimes then it is possible for natural selection to act on heritable variation in mandibular corpus morphology (under "heritable variation" we include pleiotropic effects of genetic loci [Ehrich et al., 2003, 2005] and heritable mechanisms that facilitate plastic responses to variation in strain regimes [Bouvier and Hylander, 1981, 1996a, b, 1994; Ravosa et al., 2006, 2007a, b]. This mapping from food material and geometric material properties to strain regimes is shown in Figure 12A.

This brings us to the second criterion. In order for natural selection to produce changes in mandibular corpus morphology, different mandibular corpus morphologies must perform better under different mandibular corpus stress and strain regimes, and this must improve feeding performance and fitness. For example, if relatively high bending stresses and strains associated with premolar biting are best resisted by increasing relative dorsoventral depth of the corpus, and animals with relatively deeper corpora have improved feeding performance and higher fitness, then natural selection is predicted to associate premolar biting with relatively deeper mandibular corpora. Or, if chewing foods with higher toughness is associated with relatively higher bending stresses, this might also be associated with evolution of increased depth of the mandibular corpus. As shown in Figure 12B, this can be conceived of as a weighting of the importance for mandibular morphology of the range of different oral food processing behaviors and strain regimes.

Finally, if consistent associations between oral food processing behavior, loading regime, strain regime, and corpus morphology are to evolve in different primate lineages, then these selective forces must act in the same morphological and behavioral contexts in those lineages (Kay and Cartmill, 1977; Ross et al., 2002).

The results of the experiments reported here are most germane to evaluating the first criterion discussed above: does variation in food geometric and material properties elicit variation in oral food processing behaviors, including in the way animals chew, resulting in significantly different strain regimes in the mandibular corpus? As predicted by our first hypothesis, when the three individuals in our study performed multiple different feeding behaviors using different cycle types, at the majority of sites cycle type had a significant impact on ε_1 orientations and magnitudes and on $|\varepsilon_1/\varepsilon_2|$ ratios. Food type had either weak or non-significant effects on ε_1 orientations and magnitudes, and on $|\varepsilon_1/\varepsilon_2|$ ratios, except through interaction effects with cycle type (Table 8a). As predicted by the second hypothesis, mastication was also associated with variation in strain regimes in the mandible. However, most variation was nested between cycles within chewing sequences, as reflected in cycle number and, to a lesser extent, across chewing sides. Food type had either weak or non-significant effects on strain regimes during chewing, except through chew side X food type interaction effects (Table 8b). Contrary to the third hypothesis, the most consistent effect on variation in ε_1 orientation in the mandibular corpus is variation in chewing side, the next most consistent effect is feeding behavior (including biting side): the effects of variation in food material properties on variation in strain orientations are relatively minor. Similar results are seen in *Macaca fascicularis*, where variation in mandibular corpus strain regimes across behaviors is greater than variation between chews on different foods ipsilateral or contralateral to the strain gages, but there are significant effects of chew side on strain orientations (Hylander, 1979c). These results are not unexpected because variation in the most important determinants of strain regimes in the primate mandible (jaw kinematics and relative timing of EMG activity in jaw elevator muscles) is higher within feeding sequences and across different feeding behaviors than across chews on different foods (Vinyard et al., 2008; Ross et al., 2012; Ross and Iriarte-Diaz, 2014). Together, the results presented here and the data in the literature suggest that if the morphology of the mandibular corpus reflects selection for resistance to patterns of stress and strain experienced during feeding, this morphology must be a trade-off between different behaviors, including chewing side.

It has long been recognized that mandible design reflects trade-offs in performance at a wide range of feeding and non-feeding behaviors (Hylander, 1979a, b, 1984, 2013; Daegling, 1993, 2007; Vinyard et al., 2003; Daegling and Grine, 2006; Vinyard and Ryan, 2006; Daegling and McGraw, 2007; Taylor et al., 2008; Vinyard et al., 2009; Ross et al., 2012; Ross and Iriarte-Diaz, 2014). However, in previous work, the range of feeding behaviors elicited in the

[2] Williams et al. (2011) use the term "ingestion chewing" to refer to chewing of food when it is first ingested; in contrast with "rumination chewing," which refers to chewing of regurgitated food.

laboratory during measurement of bone strain has been rather narrow. The data presented here show that when strains are recorded in animals that can use their hands during feeding, they employ a wide range of oral food processing behaviors and the mandibular corpus experiences a wide range of strain regimes (Fig. 12A). Thus, although we have not sampled the full range of food material properties encountered and processed by *Sapajus* in the wild (Wright, 2004, 2005a, b), we expect that further expansion of this study to a wider range of FMPs will be associated with a greater increase in variation in strain magnitudes and orientations associated with different food processing behaviors compared with those associated with mastication of foods with different properties.

The question of how to evaluate the relative importance for mandible design of these different behaviors and strain regimes brings us to criterion 2 (Fig. 12B). It is very difficult to directly relate variance in primate mandibular corpus morphology to ecologically relevant measures of feeding performance (e.g., short term food or nutritional intake rates), and it is impractical to relate it to fitness. Consequently, the importance of different loading regimes for mandible design has been estimated using data on strain magnitudes and inferences about the daily frequency at which different behaviors occur (Hylander, 1979c). Strain magnitude is important because very high bone strain magnitudes are associated with bone yield and fracture (Burstein et al., 1972; Reilly and Burstein, 1974, 1975), and because strain magnitude is important in triggering adaptive responses of bone remodeling, modeling, and repair (Frost, 1987, 2000; Forwood and Turner, 1995; Turner, 1998). Consequently, behaviors associated with high magnitude strain regimes may be more important determinants of mandibular form than behaviors associated with low strain behaviors. However, daily frequencies of different behaviors are also important because bones can be weakened by fatigue, so that behaviors producing lower-than-maximum strain magnitudes over long periods of time (in the case of tension) or many cycles (in the case of compression) might be as—or more—important influences on mandibular form than high strain magnitude behaviors (Carter et al., 1976, 1981; Zioupos et al., 1996, 2001). The relationships between strain magnitudes and effects of fatigue (loading time to yield or failure) in primate feeding systems are therefore crucial data to obtain, but are currently unavailable. These relationships have been studied in some human bones and for bones in several nonprimate species, but they vary among species, bones, loading regimes (Carter et al., 1981; Reilly and Currey, 1999; Zioupos et al., 2001), bone material properties (Carter et al., 1976; Currey, 2004), and temperature, so their relevance for the evolution of the primate feeding system is unclear. It is important to note that here and elsewhere (Ross et al., 2012; Ross and Iriarte-Diaz, 2014), we are not arguing that fatigue resistance has no bearing on primate mandible design, only that the nature and importance of its effects are poorly understood. What is clear is that in order to estimate the relative importance of different feeding behaviors, we need data on strain regimes (including magnitudes) for as complete a range of feeding behaviors and as wide a range of food material properties as possible, along with data on how often these behaviors are employed in the wild (Taylor et al., 2008; Vogel et al., 2014).

The results of this study also show that the largest mandibular corpus strain magnitudes were recorded during premolar and incisor bites, rather than chewing. Hylander's (1979c) data on mandibular corpus bone strain in *Macaca* and *Otolemur* also reveal higher bone strain magnitudes during isometric biting on a bite force transducer with the molars than chewing with the molars, but lower strain magnitudes during transducer biting with the incisors than ingestion incision. These results, combined with evidence that cyclic loading and long loading times can cause fatigue yielding and failure in bone, suggest that it would be valuable to know the relative proportions of time spent in biting and chewing behaviors in wild primates (Brown, 1997; Daegling and Grine, 2006; Taylor et al., 2008; Ross et al., 2012; Ross and Iriarte-Diaz, 2014).

9. Conclusions

The primate feeding behavior/feeding ecology literature is well-populated with data on the relative proportions of different items in primate diets and the proportions of time spent feeding on different items. Recent years have seen significant progress on the material and geometric properties of wild primate foods. The results of our study suggest that in order to understand the relationships between these properties and mandibular morphology, we need to know how these properties are related to and elicit different oral food processing behaviors. Data are needed on aspects of wild primate feeding behavior that impact the loading, stress and strain regimes, and histories of primate mandibles, such as where on the mandible bite forces are applied, the likely magnitudes of those forces, the gapes at which they are applied, and how many times they perform different behaviors, including number of cycles and total loading time (e.g., McGraw et al., 2011). These data need to be collected across as wide a range of behaviors as possible, including pre-ingestive, extractive feeding behaviors, such as gouging (Vinyard et al., 2001, 2003, 2009; Vinyard and Schmitt, 2004; Vinyard and Ryan, 2006) and ingestive processing, such as incisor, canine, and molar biting, in addition to chewing. Non-feeding behaviors such as threat displays (Hylander, 2013; Terhune et al., 2015) can impose significant strains on the mandible, but also impose trade-offs on feeding system design that need to be considered. Thus, the relative frequencies and importance of feeding and non-feeding will need to be factored into more complete biomechanical explanations for variation and evolution of primate feeding system form (e.g., Taylor et al., 2008).

Acknowledgements

We thank E. Vogel, N. Yamashita, and B. Wright for the opportunity to present this paper in their symposium *Food materials testing and its relevance for primate biology*, held at the 2013 Annual Meeting of the American Association of Physical Anthropologists, and for their invitation to contribute to this volume. We thank the staff of the ARC at The University of Chicago for their animal care and expertise and the reviewers of the paper for their feedback. This work was funded by National Science Foundation HOMINID and Physical Anthropology grants (BCS 0240865; BCS 0504685; BCS 0725126; BCS 0725147; BCS 0962682).

Supplementary Online Material

Supplementary online material related to this article can be found at http://dx.doi.org/10.1016/j.jhevol.2016.06.004.

References

Agrawal, K.R., Lucas, P.W., Bruce, I.C., 2000. The effects of food fragmentation index on mandibular closing angle in human mastication. Arch. Oral Biol. 45, 577–584.

Agrawal, K.R., Lucas, P.W., Prinz, J.F., Bruce, I.C., 1997. Mechanical properties of foods responsible for resisting food breakdown in the human mouth. Arch. Oral Biol. 42, 1–9.

Beecher, R.M., 1977. Function and fusion at the mandibular symphysis. Am. J. Phys. Anthropol. 47, 325–336.

Beecher, R.M., 1979. Functional significance of the mandibular symphysis. J. Morphol. 159, 117–130.

Beyron, H., 1964. Occlusal relations and mastication in Australian Aborigines. Acta Odontol. Scand. 22, 597–678.
Bouvier, M., 1986a. A biomechanical analysis of mandibular scaling in Old World monkeys. Am. J. Phys. Anthropol. 69, 473–482.
Bouvier, M., 1986b. Biomechanical scaling of mandibular dimensions in New World monkeys. Int. J. Primatol. 7, 551–567.
Bouvier, M., Hylander, W.L., 1981. Effect of bone strain on cortical bone structure in macaques (*Macaca mulatta*). J. Morphol. 167, 1–12.
Bouvier, M., Hylander, W.L., 1994. Bone remodeling responses to strain gradients in the zygomatic arch of macaques. J. Dent. Res. 73, 195.
Bouvier, M., Hylander, W.L., 1996a. The mechanical or metabolic function of secondary osteonal bone in the monkey *Macaca fascicularis*. Archs. Oral Biol. 41 (10), 941–950.
Bouvier, M., Hylander, W.L., 1996b. Strain gradients, age, and levels of modeling and remodeling in the facial bones of *Macaca fascicularis*. In: Davidovitch, Z., Norton, L.A. (Eds.), Biological Mechanisms of Tooth Movement and Craniofacial Adaptation. Harvard Society for the Advancement of Orthodontics, Boston, pp. 407–412.
Brown, B., 1997. Miocene hominoid mandibles—functional and phylogenetic perspectives. In: Begun, D.R., Ward, C.V., Rose, M.D. (Eds.), Function, Phylogeny and Fossils: Miocene Hominoid Evolution and Adaptation. Plenum, New York, pp. 153–171.
Burstein, A.H., Currey, J.D., Frankel, V.H., Reilly, D.T., 1972. The ultimate properties of bone tissue: the effects of yielding. J. Biomech. 5, 35–44.
Carter, D.R., Hayes, W.C., Schurman, D.J., 1976. Fatigue life of compact bone—II. Effects of microstructure and density. J. Biomech. 9, 211–214.
Carter, D.R., Harris, W.H., Vasu, R., Caler, W.E., 1981. The mechanical and biological response of cortical bone to in vivo strain histories. In: Cowin, S.C. (Ed.), Mechanical Properties of Bone (AMD vol. 45). American Society of Mechanical Engineers, New York, pp. 81–92.
Chalk, J., Wright, B.W., Lucas, P.W., Schuhmacher, K.D., Vogel, E.R., Fragaszy, D., Visalberghi, E., Izar, P., Richmond, B.G., 2016. Age-Related Variation in the Mechanical Properties of Foods Processed by *Sapajus libidinosus*. Am. J. Phys. Anthropol. 159, 199–209.
Cole, T.M., 1992. Postnatal heterochrony of the masticatory apparatus in *Cebus apella* and *Cebus albifrons*. J. Hum. Evol. 23, 253–282.
Currey, J.D., 2004. Tensile yield in compact bone is determined by strain, post-yield behaviour by mineral content. J. Biomech. 37, 549–556.
Daegling, D.J., 1989. Biomechanics of cross-sectional size and shape in the hominoid mandibular corpus. Am. J. Phys. Anthropol. 80, 91–106.
Daegling, D.J., 1990. Geometry and biomechanics of hominoid mandibles. Ph.D. Dissertation, State University of New York at Stony Brook.
Daegling, D.J., 1992. Mandibular morphology and diet in the genus *Cebus*. Int. J. Primatol. 13, 545–570.
Daegling, D.J., 1993. The relationship of in vivo bone strain to mandibular corpus morphology in *Macaca fascicularis*. J. Hum. Evol. 25, 247–269.
Daegling, D.J., 2002. Bone geometry in cercopithecoid mandibles. Archs. Oral Biol. 47, 315–325.
Daegling, D.J., 2007. Relationship of bone utilization and biomechanical competence in hominoid mandibles. Archs. Oral Biol. 52, 51–63.
Daegling, D.J., 2012. The Human Mandible and the Origins of Speech. J. Anthropol. 2012, 201502 http://dx.doi.org/10.1155/2012/201502, 14 pages.
Daegling, D.J., Grine, F.E., 2006. Mandibular biomechanics and the paleontological evidence for the evolution of human diet. In: Ungar, P.S. (Ed.), Evolution of the Human Diet: The Known, the Unknown, and the Unknowable. Oxford University Press, Cary, pp. 77–105.
Daegling, D.J., McGraw, W.S., 2001. Feeding, diet, and jaw form in West African *Colobus* and *Procolobus*. Int. J. Primatol. 22, 1033–1055.
Daegling, D.J., McGraw, W.S., 2007. Functional morphology of the mangabey mandibular corpus: Relationship to dental specializations and feeding behavior. Am. J. Phys. Anthropol. 134, 50–62.
Demes, B., 1998. Use of strain gauges in the study of primate locomotor biomechanics. In: Strasser, E., Fleagle, J., Rosenberger, A., McHenry, H. (Eds.), Primate Locomotion. Recent Advances. Plenum Press, New York, pp. 237–254.
Demes, B., 2007. In vivo bone strain and bone functional adaptation. Am. J. Phys. Anthropol. 133, 717–722.
Demes, B., Qin, Y.X., Stern, J.T., Larson, S.G., Rubin, C.T., 2001. Patterns of strain in the macaque tibia during functional activity. Am. J. Phys. Anthropol. 116, 257–265.
Ehrich, T.H., Vaughn, T.T., Koreishi, S.F., Linsey, R.B., Pletscher, L.S., Cheverud, J.M., 2003. Pleiotropic effects on mandibular morphology I. Developmental morphological integration and differential dominance. J. Exp. Zool. B Mol. Dev. Evol. 296, 58–79.
Ehrich, T.H., Kenney-Hunt, J.P., Pletscher, L.S., Cheverud, J.M., 2005. Genetic variation and correlation of dietary response in an advanced intercross mouse line produced from two divergent growth lines. Genet. Res. 85, 211–222.
Ekfeldt, A., Karlsson, S., 1996. Changes of masticatory movement characteristics after prosthodontic rehabilitation of individuals with extensive tooth wear. Int. J. Prosthodont. 9, 539–546.
Eng, C.M., Ward, S.R., Vinyard, C.J., Taylor, A.B., 2009. The morphology of the masticatory apparatus facilitates muscle force production at wide jaw gapes in tree-gouging common marmosets (*Callithrix jacchus*). J. Exp. Biol. 212, 4040–4055.
Fisher, N.I., 1993. Statistical Analysis of Circular Data. Cambridge University Press, New York.
Forwood, M.R., Turner, C.H., 1995. Skeletal adaptations to mechanical usage: Results from tibial loading studies in rats. Bone 17, 197S–205S.
Frost, H.M., 1987. The mechanostat: a proposed pathogenic mechanism of osteoporoses and the bone mass effects of mechanical and nonmechanical agents. Bone Min. 2, 73–85.
Frost, H.M., 2000. Why the ISMNI and the Utah paradigm? Their role in skeletal and extraskeletal disorders. J. Musculoskel. Neuronal Interact 1, 5–9.
Hiiemae, K.M., 1976. Masticatory movements in primitive mammals. In: Anderson, D.J., Matthews, B. (Eds.), Mastication. John Wright & Sons Ltd., Bristol, pp. 105–118.
Hiiemae, K.M., 1978. Mammalian mastication: a review of the activity of jaw muscles and the movements they produce in chewing. In: Butler, P.M., Joysey, K. (Eds.), Development, Function and Evolution of Teeth. Academic Press, London, pp. 359–398.
Hiiemae, K.M., 2000. Feeding in mammals. In: Schwenk, K. (Ed.), Feeding: Form, Function and Evolution in Tetrapod Vertebrates. Academic Press, London, pp. 411–457.
Hildebrand, G.Y., 1931. Studies in the masticatory movements of the human lower jaw. Skandinavisches Archiv Fur Physiologie 61. COVER1–190.
Hylander, W.L., 1979a. An experimental analysis of temporomandibular joint reaction force in macaques. Am. J. Phys. Anthropol. 51, 433–456.
Hylander, W.L., 1979b. The functional significance of primate mandibular form. J. Morphol. 160, 223–240.
Hylander, W.L., 1979c. Mandibular function in *Galago crassicaudatus* and *Macaca fascicularis*: An in vivo approach to stress analysis of the mandible. J. Morphol. 159, 253–296.
Hylander, W.L., 1984. Stress and strain in the mandibular symphysis of primates: A test of competing hypotheses. Am. J. Phys. Anthropol. 64, 1–46.
Hylander, W.L., 1988. Implications of in vivo experiments for interpreting the functional significance of "robust" australopithecine jaws. In: Grine, F.E. (Ed.), Evolutionary History of the "Robust" Australopithecines. Aldine de Gruyter, New York, pp. 55–83.
Hylander, W.L., 2013. Functional links between canine height and jaw gape in catarrhines with special reference to early hominins. Am. J. Phys. Anthropol. 150, 247–259.
Hylander, W.L., Bays, R., 1979. In vivo strain gauge analysis of the dentary squamosal joint reaction force during mastication and incisal biting in *Macaca mulatta* and *Macaca fascicularis*. Archs. Oral Biol. 24, 689–697.
Hylander, W.L., Johnson, K.R., 1994. Jaw muscle function and wishboning of the mandible during mastication in macaques and baboons. Am. J. Phys. Anthropol. 94, 523–547.
Hylander, W.L., Johnson, K.R., Crompton, A.W., 1987. Loading patterns and jaw movements during mastication in *Macaca fascicularis*: A bone-strain, electromyographic, and cineradiographic analysis. Am. J. Phys. Anthropol. 72, 287–314.
Hylander, W.L., Ravosa, M.J., Ross, C.F., Johnson, K.R., 1998. Mandibular corpus strain in Primates: Further evidence for a functional link between symphyseal fusion and jaw-adductor muscle force. Am. J. Phys. Anthropol. 107, 257–271.
Ingervall, B., 1972. Tooth contacts on the functional and nonfunctional side in children and young adults. Arch. Oral Biol. 17, 191–200.
Iriarte-Diaz, J., Reed, D.A., Ross, C.F., 2011. Sources of variance in temporal and spatial aspects of jaw kinematics in two species of primates feeding on foods of different properties. Integr. Comp. Biol. 51, 307–319.
Kay, R.F., Cartmill, M., 1977. Cranial morphology and adaptations of *Palaechthon nacimienti* and other Paromomyidae (Plesiadapoidea? Primates), with a description of a new genus and species. J. Hum. Evol. 6, 19–35.
Kimbel, W.H., Johanson, D., Rak, Y., 2004. The Skull of *Australopithecus afarensis*. Oxford University Press, Oxford.
Lynch-Alfaro, J.W., Silva, J.D.E., Rylands, A.B., 2012. How different are robust and gracile capuchin monkeys? An argument for the use of *Sapajus* and *Cebus*. Am. J. Primatol. 74, 273–286.
Mardia, K.V., Jupp, P.E., 2000. Directional Statistics. Wiley, Chichester.
McGraw, W.S., Vick, A.E., Daegling, D.J., 2011. Sex and Age Differences in the Diet and Ingestive Behaviors of Sooty Mangabeys (*Cercocebus atys*) in the Tai Forest, Ivory Coast. Am. J. Phys. Anthropol. 144, 140–153.
Ravosa, M.J., 1991. Structural allometry of the mandibular corpus and symphysis in prosimian primates. J. Hum. Evol. 20, 3–20.
Ravosa, M.J., 1992. Allometry and heterochrony in extant and extinct Malagasy primates. J. Hum. Evol. 23, 197–217.
Ravosa, M.J., 1996. Jaw morphology and function in living and fossil Old World Monkeys. Int. J. Primatol. 17, 909–932.
Ravosa, M.J., 2000. Size and scaling in the mandible of living and extinct apes. Folia Primatol. 71, 305–322.
Ravosa, M.J., 2007. Cranial ontogeny, diet, and ecogeographic variation in African lorises. Am. J. Primatol. 69, 59–73.
Ravosa, M.J., Nicholson, E.K., Stock, S.R., Hamrick, M.W., 2006. Biomineralization and adaptive plasticity of the temporomandibular joint in myostatin knockout mice. Archs. Oral Biol. 51, 37–49.
Ravosa, M.J., Klopp, E.B., Pinchoff, J., Stock, S.R., Hamrick, M.W., 2007a. Plasticity of mandibular biomineralization in myostatin-deficient mice. J. Morphol. 268, 275–282.
Ravosa, M.J., Kunwar, R., Stock, S.R., Stack, M.S., 2007b. Pushing the limit: masticatory stress and adaptive plasticity in mammalian craniomandibular joints. J. Exp. Biol. 210, 628–641.
Reed, D.A., Ross, C.F., 2010. The influence of food material properties on jaw kinematics in the primate, *Cebus*. Archs. Oral Biol. 55, 946–962.

Reilly, D.T., Burstein, A.H., 1974. Review article. The mechanical properties of cortical bone. J. Bone Joint Surg. 56, 1001–1022.
Reilly, D.T., Burstein, A.H., 1975. The elastic and ultimate properties of compact bone tissue. J. Biomech. 8, 393–405.
Reilly, G.C., Currey, J.D., 1999. The development of microcracking and failure in bone depends on the loading mode to which it is adapted. J. Exp. Biol. 202, 543–552.
Rilo, B., Fernandez-Formoso, N., Mora, M.J., Cadarso-Suarez, C., Santana, U., 2009. Distance of the contact glide in the closing masticatory stroke during mastication of three types of food. J. Oral Rehabil. 36, 571–576.
Ross, C.F., Iriarte-Diaz, J., 2014. What does feeding system morphology tell us about feeding? Evol. Anthropol. 23, 105–120.
Ross, C.F., Metzger, K.A., 2004. Bone strain gradients and optimization in tetrapod skulls. Ann. Anat. 186, 387–396.
Ross, C.F., Lockwood, C.A., Fleagle, J.G., Jungers, W.L., 2002. Adaptation and behavior in the primate fossil record. In: Plavcan, J.M., Kay, R.F., Jungers, W.L., van Schaik, C.P. (Eds.), Reconstructing Behavior in the Primate Fossil Record. Kluwer Academic/Plenum Publishers, New York, pp. 1–41.
Ross, C.F., Iriarte-Diaz, J., Nunn, C.L., 2012. Innovative approaches to the relationship between diet and mandibular morphology in primates. Int. J. Primatol. 33, 632–660.
Ross, C.F., Washington, R.L., Eckhardt, A., Reed, D.A., Vogel, E.R., Dominy, N.J., Machanda, Z.P., 2009. Ecological consequences of scaling of chew cycle duration and daily feeding time in Primates. J. Hum. Evol. 56, 570–585.
Rybicki, E.F., Mills, E.J., Turner, A.S., Simonen, F.A., 1977. *In vivo* and analytical studies of forces and moments in equine long bones. J. Biomech. 10, 701–705.
Smith, R.J., 1984. Comparative functional morphology of maximum mandibular opening (gape) in primates. In: Chivers, D.J., Wood, B.A., Bilsborough, A. (Eds.), Food Acquisition and Processing in Primates. Plenum Press, New York, pp. 231–255.
Suit, S.R., Gibbs, C.H., Benz, S.T., 1976. Study of gliding tooth contacts during mastication. J. Periodontol. 47, 331–334.
Taylor, A.B., 2002. Masticatory form and function in the African apes. Am. J. Phys. Anthropol. 117, 133–156.
Taylor, A.B., 2006a. Diet and mandibular morphology in African apes. Int. J. Primatol. 27, 181–201.
Taylor, A.B., 2006b. Feeding behavior, diet, and the functional consequences of jaw form in orangutans, with implications for the evolution of *Pongo*. J. Hum. Evol. 50, 377–393.
Taylor, A.B., Vinyard, C.J., 2009. Jaw-muscle fiber architecture in tufted capuchins favors generating relatively large muscle forces without compromising jaw gape. J. Hum. Evol. 57, 710–720.
Taylor, A.B., Vogel, E.R., Dominy, N.J., 2008. Food material properties and mandibular load resistance abilities in large-bodied hominoids. J. Hum. Evol. 55, 604–616.
Terhune, C.E., Hylander, W.L., Vinyard, C.J., Taylor, A.B., 2011. Masseter fiber length and position influence relative maximum jaw gapes in the sexually-dimorphic *Macaca fascicularis*. Am. J. Phys. Anthropol. 144, 292.
Terhune, C.E., Hylander, W.L., Vinyard, C.J., Taylor, A.B., 2015. Jaw-muscle architecture and mandibular morphology influence relative maximum jaw gapes in the sexually dimorphic *Macaca fascicularis*. J. Hum. Evol. 82, 145–158.
Theriault, B.R., Reed, D.A., Niekrasz, M.A., 2008. Reversible medetomidine/ketamine anesthesia in captive capuchin monkeys (*Cebus apella*). J. Med. Primatol. 37, 74–81.
Turner, C.H., 1998. Three rules for bone adaptation to mechanical stimuli. Bone 23, 399–407.
Van Soest, P.J., 1996. Allometry and ecology of feeding behavior and digestive capacity in herbivores: A review. Zoo Biol. 15, 455–479.
Vinyard, C.J., Ryan, T.M., 2006. Cross-sectional bone distribution in the mandibles of gouging and non-gouging Platyrrhini. Int. J. Primatol 27, 1461–1490.
Vinyard, C.J., Schmitt, D., 2004. New technique for studying reaction forces during primate behaviors on vertical substrates. Am. J. Phys. Anthropol. 125, 343–351.
Vinyard, C.J., Wall, C.E., Williams, S.H., Schmitt, D., Hylander, W.L., 2001. A preliminary report on the jaw mechanics during tree gouging in common marmosets (*Callithrix jacchus*). In: Brooks, A. (Ed.), Dental morphology 2001: Proceedings of the 12th International Symposium on Dental Morphology. Sheffield Academic Press, Sheffield, pp. 283–297.
Vinyard, C.J., Wall, C.E., Williams, S.H., Hylander, W.L., 2003. Comparative functional analysis of skull morphology of tree-gouging primates. Am. J. Phys. Anthropol. 120, 153–170.
Vinyard, C.J., Wall, C.E., Williams, S.H., Hylander, W.L., 2008. Patterns of variation across primates in jaw-muscle electromyography during mastication. Integr. Comp. Biol. 48, 294–311.
Vinyard, C.J., Wall, C.E., Williams, S.H., Mork, A.L., Armfield, B.A., Melo, L.C.D., Valenca-Montenegro, M.M., Valle, Y.B.M., de Oliveira, M.A.B., Lucas, P.W., Schmitt, D., Taylor, A.B., Hylander, W.L., 2009. The evolutionary morphology of tree gouging in marmosets. In: Ford, S.M., Porter, L.M., Davis, L.C. (Eds.), The Smallest Anthropoids: The Marmoset/Callimico Radiation. Springer, New York, pp. 395–409.
Vogel, E.R., Zulfa, A., Hardus, M., Wich, S.A., Dominy, N.J., Taylor, A.B., 2014. Food mechanical properties, feeding ecology, and the mandibular morphology of wild orangutans. J. Hum. Evol. 75, 110–124.
Wallisch, P., Lusignan, M., Benayoun, M., Baker, T.I., Dickey, A.S., Hatsopoulos, N.G., 2009. Matlab (R) for Neuroscientists: An Introduction to Scientific Computing in Matlab (R). Elsevier, San Diego.
Weijs, W.A., De Jong, J.H., 1977. Strain in mandibular alveolar bone during mastication in the rabbit. Archs. Oral Biol. 22, 667–675.
Williams, S.H., Stover, K.K., Davis, J.S., Montuelle, S.J., 2011. Mandibular corpus bone strains during mastication in goats (*Capra hircus*): A comparison of ingestive and rumination chewing. Archs. Oral Biol. 56, 960–971.
Williams, S.H., Wright, B.W., Den Truong, V., Daubert, C.R., Vinyard, C.J., 2005. Mechanical properties of foods used in experimental studies of primate masticatory function. Am. J. Primatol. 67, 329–346.
Woda, A., Vigneron, P., Kay, D., 1979. Non-functional and functional occlusal contacts – Review of the literature. J. Prosthet. Dent. 42, 335–341.
Woltring, H.J., Huiskes, R., de Lange, A., Veldpaus, F.E., 1985. Finite centroid and helical axis estimation from noisy landmark measurements in the study of human joint kinematics. J. Biomech. 18, 379.
Wright, B.W., 2004. Food mechanical properties and niche partitioning in a community of Neotropical primates. Am. J. Phys. Anthropol. 212.
Wright, B.W., 2005a. Craniodental biomechanics and dietary toughness in the genus *Cebus*. J. Hum. Evol. 48, 473–492.
Wright, B.W., 2005b. Dietary demand and niche breadth among six primates in Guyana, South America. Am. J. Phys. Anthropol. (Suppl. 40), 227.
Wright, B.W., Wright, K.A., Chalk, J., Verderane, M.P., Fragaszy, D., Visalberghi, E., Izar, P., Ottoni, E.B., Constantino, P., Vinyard, C.J., 2009. Fallback foraging as a way of life: Using dietary toughness to compare the fallback signal among capuchins and implications for interpreting morphological variation. Am. J. Phys. Anthropol. 140, 687–699.
Wright, K.A., Wright, B.W., Ford, S.M., Fragaszy, D., Izar, P., Norconk, M., Masterson, T., Hobbs, D.G., Alfaro, M.E., Alfaro, J.W.L., 2015. The effects of ecology and evolutionary history on robust capuchin morphological diversity. Mol. Phylogenet. Evol. 82, 455–466.
Zioupos, P., Xiao, T.W., Currey, J.D., 1996. Experimental and theoretical quantification of the development of damage in fatigue tests of bone and antler. J. Biomech. 29, 989–1002.
Zioupos, P., Currey, J.D., Casinos, A., 2001. Tensile fatigue in bone: Are cycles-, or time to failure, or both, important? J. Theor. Biol. 210, 389.